

# Deliverable D28 (D4.7)

Summary: mapping procedures, sustainability and applicability for upscaling



RI-URBANS

Research Infrastructures Services Reinforcing Air  
Quality Monitoring Capacities in European Urban &  
Industrial Areas (GA n. 101036245)

By

UU, VITO, UoB, DCMR, CNRS-ENPC, INOE, FMI, NOA & UHEL



UNIVERSITY OF  
BIRMINGHAM



16/01/2025

**Deliverable D28 (D4.7): Summary: mapping procedures, sustainability and applicability for upscaling**

Authors: Gerard Hoek (UU), Jules Kerckhoffs (UU), Martine van Poppel (VITO), Jelle Hofman (VITO), Roy Harrison (UoB), Dimitrios Boutrios (UoB), Sef van den Elshout (DCMR), Karine Sartelet (CNRS-ENPC), Jeni Vasilescu (INOE), Hilikka Timonen (FMI), Juha Kangasluoma (UHEL) & Tuukka Petäjä (UHEL)

<b>Work package (WP)</b>	WP4 Pilot implementations for testing and demonstrating services
<b>Deliverable</b>	D28 (D4.7)
<b>Lead beneficiary</b>	UU
<b>Deliverable type</b>	<input checked="" type="checkbox"/> R (document, report) <input type="checkbox"/> DEC (websites, patent filings, videos,...) <input type="checkbox"/> Other: ORDP (open research data pilot)
<b>Dissemination level</b>	<input checked="" type="checkbox"/> PU (public) <input type="checkbox"/> CO (confidential, only members of consortium and European Commission)
<b>Estimated delivery deadline</b>	M40 (31/01/2025)
<b>Actual delivery deadline</b>	16/01/2025
<b>Version</b>	Final
<b>Reviewed by</b>	WP4 leaders and project coordinators
<b>Accepted by</b>	RI-URBANS Project Coordination Team
<b>Comments</b>	<p>This report summarizes experiences in RI-urbans pilot studies with complementary approaches to traditional AQMS in order to derive high-resolution air pollution exposure maps for epidemiological studies, source evaluation and to assess policy actions at urban scale. The pilot studies built on guidelines in WP2 deliverable 2.5 for the empirical modelling and WP3 for the dispersion modelling. Generally positive experiences were obtained with the proposed methodology, with some modifications to improve. We finish with a reflection on upscaling and sustainability.</p>

## Table of Contents

<b>1. ABOUT THIS DOCUMENT</b> .....	<b>1</b>
<b>2. AIMS OF THE DELIVERABLE</b> .....	<b>2</b>
<b>3. BIRMINGHAM PILOTS</b> .....	<b>2</b>
3.1 LOW-COST SENSOR MONITORING .....	2
3.2 AIR QUALITY ASSESSMENT AT NEIGHBOURHOOD SCALE .....	3
3.3 STREET LEVEL AIR QUALITY ASSESSMENT AND POLLUTION SOURCE APPORTIONMENT .....	5
3.4 PREDICTING PM <sub>2.5</sub> CONCENTRATIONS .....	7
3.5 GAUSSIAN-BASED DISPERSION MODELLING APPROACH WITH THE ADMS-URBAN MODEL OVER BIRMINGHAM .....	9
<b>4. ROTTERDAM: CITIZEN-BASED MOBILE MONITORING</b> .....	<b>11</b>
4.1. MONITORING STRATEGY .....	11
4.2 ACCURACY .....	11
4.3 NORMALIZATION.....	12
4.4 NUMBER OF REPEATS.....	13
<b>5. ROTTERDAM CAR-BASED MOBILE MONITORING</b> .....	<b>13</b>
5.1. MONITORING STRATEGY .....	13
5.2 NUMBER OF REPEATS.....	14
5.3 VALIDATION .....	15
5.4 MAPS .....	15
<b>6. BUCHAREST PILOT</b> .....	<b>18</b>
6.1 MOBILE MEASUREMENTS AND DATA .....	18
6.2 MODEL .....	19
6.3 MAPS BASED ON CAR MEASUREMENTS .....	19
6.4 VARIABILITY WITHIN 1 KM X 1KM AREAS .....	21
6.5 SUMMARY .....	21
<b>7. PARIS PILOT</b> .....	<b>22</b>
7.1 EULERIAN APPROACH WITH THE CHIMERE/MUNICH/SSH-AEROSOL CHAIN OVER PARIS .....	22
7.2 HYBRID APPROACH WITH THE CHIMERE/ADMS CHAIN OVER PARIS.....	26
<b>8. ATHENS PILOT</b> .....	<b>32</b>
8.1 COMPARISON OF SUMMER AND WINTER CONCENTRATIONS .....	33
<b>9. HELSINKI PILOTS</b> .....	<b>36</b>
9.1 KUMPULA BC-SENSOR CAMPAIGN .....	37
9.2 BIKE CAMPAIGN .....	39
9.3 LESSONS LEARNED FROM THE HELSINKI AQ MAPPING ACTIVITIES .....	41
<b>9. POTENTIAL FOR SUSTAINABILITY AND UPSCALING IN CITIES</b> .....	<b>41</b>
<b>10. REFERENCES</b> .....	<b>43</b>

## 1. ABOUT THIS DOCUMENT

Two approaches have been adopted in the pilot studies to develop high spatial resolution maps of outdoor air pollutants across cities. The first approach involves statistical models (land use regression) derived from measured concentrations. The second methodology that has been used to develop spatial maps is high-resolution dispersion modelling. The pollutants that have been covered in the pilots include Ultra Fine Particles (UFP), Black Carbon (BC), nitrogen dioxide (NO<sub>2</sub>), particle mass concentrations (PM) smaller than 2.5 µm and 10 µm (PM<sub>2.5</sub>, PM<sub>10</sub>). This document takes advantage of developed [STs](#) (from WP1-3) to describe the variability of outdoor exposure of nanoparticles and other pollutants using modelling tools, mobile measurements of nanoparticles, BC and PM mid-cost sensors, novel dispersion modelling. The approaches for fine scale mapping will be evaluated for their potential for upscaling and sustainable implementation in cities in this deliverable D28 (D4.7)

As outlined in the RI-URBANS [Deliverable D13 \(D2.5\)](#), improved spatiotemporal resolution of multi-component air quality (AQ) data is critical for improved understanding of the connection between AQ parameters, human exposure and consequent health effects. Advances in sensor technologies and the availability of portable and sensing devices give rise to new opportunities for mobile monitoring and denser fixed sensor networks, compared to the current spatially sparse, temporally rich routine monitoring. More specifically, [D13 \(D2.5\)](#) summarized complementary approaches to traditional AQMS in order to derive high-resolution exposure maps based on monitoring data. These monitoring approaches were subsequently tested in three RI-URBANS pilot cities as part of WP4. Specifically, pilots were conducted in the cities Birmingham (UK), Rotterdam (The Netherlands) and Bucharest (Romania). The lessons learned from these pilot city initiatives are compiled in Deliverable D14 (D2.6). The current deliverable focusses more on the results, including validation of modelling approaches. Deliverable D27 has already described some results of the pilot studies discussed here, focusing on variability of concentrations between seasons and variability within 1\*1 km grids. A summary is provided in the current deliverable.

In Birmingham, an ADMS numerical model was developed in which street-scale dispersion was given with an ultimate resolution of 10x10 m, validated using data from a dense local sensor network supplemented with citizens monitoring for PM<sub>2.5</sub>, BC, NO<sub>2</sub> and nanoparticles. In Paris, mapping was provided using two modelling approaches:

CHIMERE coupled to ADMS with data assimilation for NO<sub>2</sub>, PM<sub>10</sub>, BC, and multi-scale modelling with CHIMERE coupled to the street model MUNICH for NO<sub>2</sub>, PM<sub>2.5</sub>, PM<sub>10</sub>, nanoparticles, BC, inorganic and organic aerosols.

The pilots partly address different issues and use different approaches. This was a deliberate choice to increase the experiences from the different approaches.

This document is delivered to the European Commission as RI-URBANS deliverable D14 (D4.7) and shared with all RI-URBANS partners for their use. It will also be made available in the public domain, <https://riurbans.eu/work-package-4/#deliverables-wp4>.

## 2. AIMS OF THE DELIVERABLE

The aim of this Deliverable D14 (D4.7) is to present:

- Summary of the pilot studies, including methods, results (maps, statistics), validation and required resources.
- Potential for upscaling and sustainable implementation in cities

We first discuss results per pilot (Birmingham, Rotterdam, Bucharest, Paris and Athens) and then present an overall assessment.

## 3. BIRMINGHAM PILOTS

In the Birmingham pilot, both monitoring and dispersion modelling has been performed. Monitoring included citizen-involved approaches using low-cost sensors.

### 3.1 Low-cost sensor monitoring

We tried several approaches using low-cost sensors (LCS) and citizen involvement for monitoring AQ and identifying the sources of pollution in Selly Oak, a residential area near the University of Birmingham (UK) and about 3 km south-west from the city center. The main study area was a residential block of about 1 km<sup>2</sup>, though in some monitoring activities additional area was covered. This area is of great interest as it is the home of about 10,000 residents, who are mostly students at the University. The main measuring period was in the spring and summer of 2023, though some additional measurements were also done in the autumn of 2022. The main low-cost sensor used was the Alphasense OPC-N3, measuring PM (PM<sub>1</sub>, PM<sub>2.5</sub> and PM<sub>10</sub>) as well as particle counts in 24 size bins in the range between 0.35-40 µm, with a resolution of 10 seconds. The OPC-N3 is an optical particle counter and can measure particle counts up to 10,000 particles/cm<sup>3</sup>. The PM accuracy of the sensor, as reported by the manufacturer, is lower than 1 µg /m<sup>3</sup> and the PM range measured is between 0 and 2000 µg /m<sup>3</sup>. The main setup also included a sensor collecting meteorological data (Bosch BME-280), namely relative humidity (RH) (used for the calibration of the sensors), temperature and atmospheric pressure, a GPS module for geolocation and a GSM module for rapid reporting.

Additionally, for specific monitoring activities we used a medium -cost sensor for BC measurements (MAGEE microAeth AE51) measuring in a varying resolution between 10 seconds to 1 minute (according to the environment and conditions). This sensor measures the rate of absorption of transmitted light (880 nm) due to continuous collection of aerosol deposit on a filter. Using the changes in absorption rate the sensor internally calculates and reports the BC concentrations (hence, it is reported as equivalent BC (eBC) in some studies). The measurement range is 0 – 1 mg BC m<sup>-3</sup> and the precision is ±0.1 µg BC m<sup>-3</sup>. The device comes with its own rechargeable battery which can power the device for about 2 days.

The calibration of the low-cost sensors was done by collocating them to the research grade instruments at the Birmingham Air Quality Supersite (BAQS). The OPC-N3, as most low-cost PM sensors, suffers in high humidity conditions, reporting higher PM concentrations, especially for the larger PM. Thus, for their calibration, after excluding the outliers which bias the calibration process, an exponential regression was applied, considering the effect of the relative humidity. This greatly improved the performance of the sensors, achieving for the PM<sub>10</sub>  $r > 0.60$ , while performing a lot better for the smaller sized PM. The BC sensor did not appear to be greatly affected by the environmental conditions, and thus, a linear regression was sufficient to improve its performance.

Finally, for specific projects the Testo DiSCmini was also used. While its price is higher than the other low-cost sensors used, it is still significantly cheaper than its research grade counterparts. The Testo DiSCmini, is a hand-held ultrafine particle counter measuring the number and average diameter of nanoparticles (10 to 700 nm) based on the electrical charge of aerosols. The sensor measures particle counts between 1,000 – 1,000,000 particles  $\text{cm}^{-3}$  with an accuracy of  $\pm 100$  particles  $\text{cm}^{-3}$ . Apart from the particle number, the DiSCmini reports the Lung Deposited Surface Area (LDSA) of particles, a metric used in health studies, as it is considered more important than the PM concentrations to portray the health effect of air pollution. The sensor comes with its own rechargeable battery which can power the device for about 9 hours.

Using multiple setups with these sensors, we collected data from static points (indoors and outdoors) as well as mobile measurements using either walks or cycle sessions in the study area. For both the static and mobile measurements we asked for the help of the local community, setting up sensors at schools and local businesses, as well as of students at the University. The projects will be discussed separately in detail in the following chapters. The aims of the projects were to elucidate the capabilities of low-cost sensors for the extension of the current measuring network, indoor air quality assessment and identification of air pollution sources. Partial aims of the projects will be discussed in each separate chapter.

### 3.2 Air quality assessment at neighbourhood scale

#### Monitoring

We set up 6 static measuring points in the study area in which we installed an OPC-N3 as well as the BC monitor (in two points). The BC sensor was used at the traffic site, as well as at the BAQS (a background site). The points were strategically chosen to cover as much of the studied area as possible, while also collecting data from points of interest. One sampling point was the BAQS, in which the OPC-N3 and BC sensors were placed next to the research grade instruments for quality control and calibration. In addition, we setup sites next to the main road in the area (Bristol Road) to measure traffic emissions, at 2 elementary schools in the block, a local business located within the area with the greatest activity (including markets, restaurants, etc.) and outside a house in the center of the study area and next to the train station. Data was collected for a total period of 3 months, between April and June 2023. Three setups were used for this campaign (Figure 1):

- Two OPC-N3 with the additional sensors using mains for powering;
- Two OPC-N3 with the additional sensors and a BC sensor using mains for powering,
- Two OPC-N3 with the additional sensors powered by a car battery. This setup was powered for about 25 days. An additional car battery was interchanged between the setups to eliminate the charging period.



Figure 1. From left to right, the three setups used for monitoring.

### *Data processing*

While data was collected in 10 second intervals, they were averaged to 1 hour, as this study focused on long-term monitoring. Average, minimum and maximum PM and BC concentrations were reported after calibrated against the research grade instruments at the BAQS. The collocation and calibration were done both at the beginning and the end of the campaign, assuring at least 2 days of simultaneous measurements. To ensure the best calibration possible, outliers (mostly due to the hygroscopicity effect mentioned in the Overview section above) were removed from the obtained dataset (about 5% of the total measurements). This approach was chosen as the inclusion of extreme outliers tended to negatively impact the calibration of the measurements from the OPC-N3. Furthermore, while the meteorological sensors provided data which were used for calibrating and reporting, wind data from the meteorological station at the BAQS were used. No additional steps were needed for data processing.

### *Results*

The obtained results included the assessment of the air quality at neighborhood scale within the study area. As 5 measuring points (sites) were located within an area of just 1 km<sup>2</sup> (plus one more collocated with the research grade instruments at the BAQS), fine spatial resolution was achieved and the effect of local sources of pollution was considered (Figure 2). Additionally, the effect of the meteorological conditions on the air quality, as well as the temporal variation of the pollutants measured were considered and reported. Finally, the long-term performance of the low-cost sensors against research grade instruments for pollution monitoring was assessed.

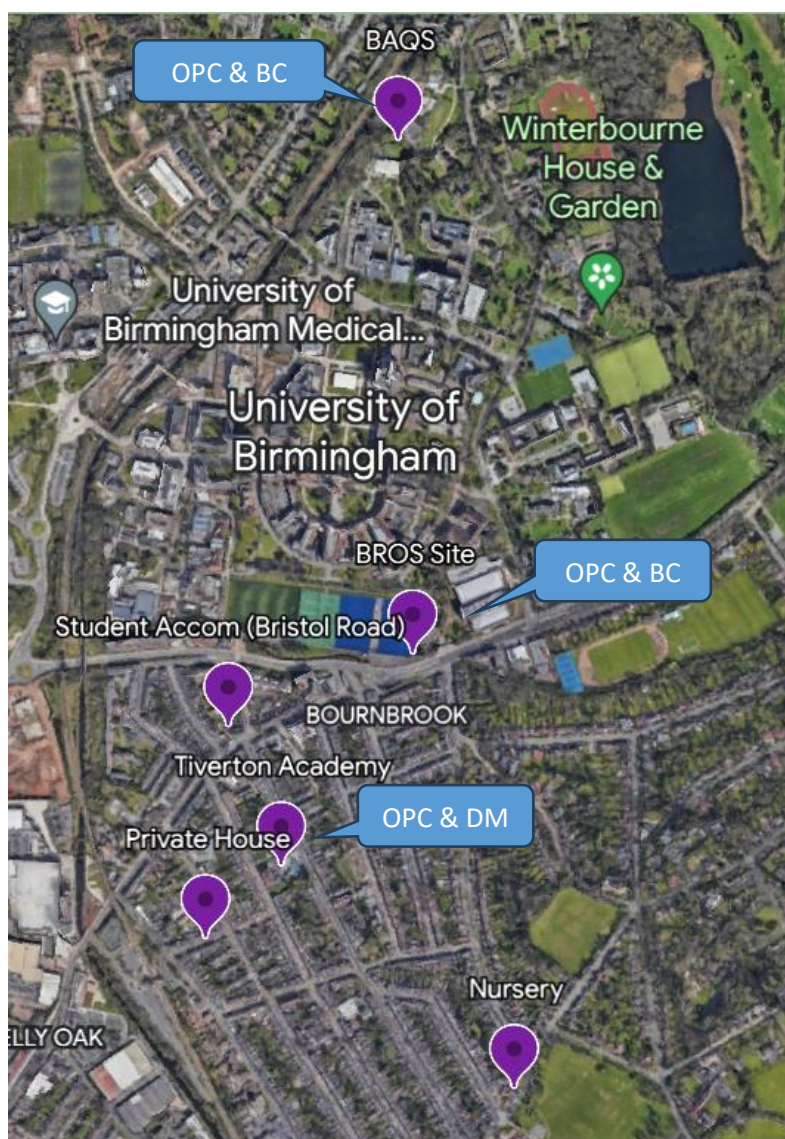


**Figure 2.** Map of the static measuring sites. An Alphasense OPC-N3 was used at all sites, while the sites indicated used an additional sensor (BC stands for the Aethlabs AE51 aethalometer and DM stands for the Testo Diskmini).

### 3.3 Street level air quality assessment and pollution source apportionment

#### Monitoring

For this campaign, two different approaches were used. First, walking sessions were done within the main block, in different times of the day following a specific route covering all the roads of the block. Second, a number of cycling sessions covering a larger area were done in different times of the day. In total, 51 walks and 34 cycling sessions were done. The setup used in this case included the OPC-N3 and the additional sensors carried within a backpack and powered by a USB power bank (figure 3). The specific setup can be powered using the power bank for about 2 days, easily sufficient for the needs of each session. In some walking or cycling sessions the Testo DISCmini and/or the BC sensor were also used. As the sensors are small in size and lightweight, the whole setup only occupied the shoe compartment of the backpack allowing for the rest of the bag to be normally used without adding too much weight.



Monitoring was done by students at the University, both PhD and MSc, as well as by a Postdoctoral researcher who was also overseeing the campaign. The campaign was advertised to the MSc students of the Air Pollution Management and Control at the University of Birmingham. A payment was included to promote the offer. For the PhD students and the Postdoctoral researcher no payment was included as it was part of the student's research.



**Figure 3.** Mobile OPC-N3 setup. The sensors were put in the shoe compartment, leaving the rest of the backpack space free, and were powered by a power bank. There was enough space for additional sensors if needed. The total added weight was less than 1 kg.

### Data processing

For the data processing, extra care was taken on the averaging of the data. As several different sensors were used, there were different time scales. All data were averaged to 10 second interval averages, which, for the walking sessions, represented a distance of about 15-20 meters. Similarly, the GPS data were also averaged in the same manner. When maps were created using such data, extra care was taken to avoid misalignments due to change of direction while walking or cycling. This is a very important consideration, as GPS data that are not correctly averaged may result in erroneous results.

### Results

With this data, we were able to report concentrations and variations, both temporal and spatial, at street level. Furthermore, the data from the walking sessions were used for a source apportionment study (Bousiotis et al., 2024). For this, PM, BC and Lung Deposited Surface Area (LDSA) data from 10 walks were used (these 10 walks were done by a single person following the same route and using the same sensors every time). Using this data the variable effect of both regional and local sources within the study area was calculated in fine detail (about 100m X 100m). Furthermore, the extent of the effect of point sources was also considered providing valuable information for potential public health studies of hyperlocal sources of pollution (Figure 4).

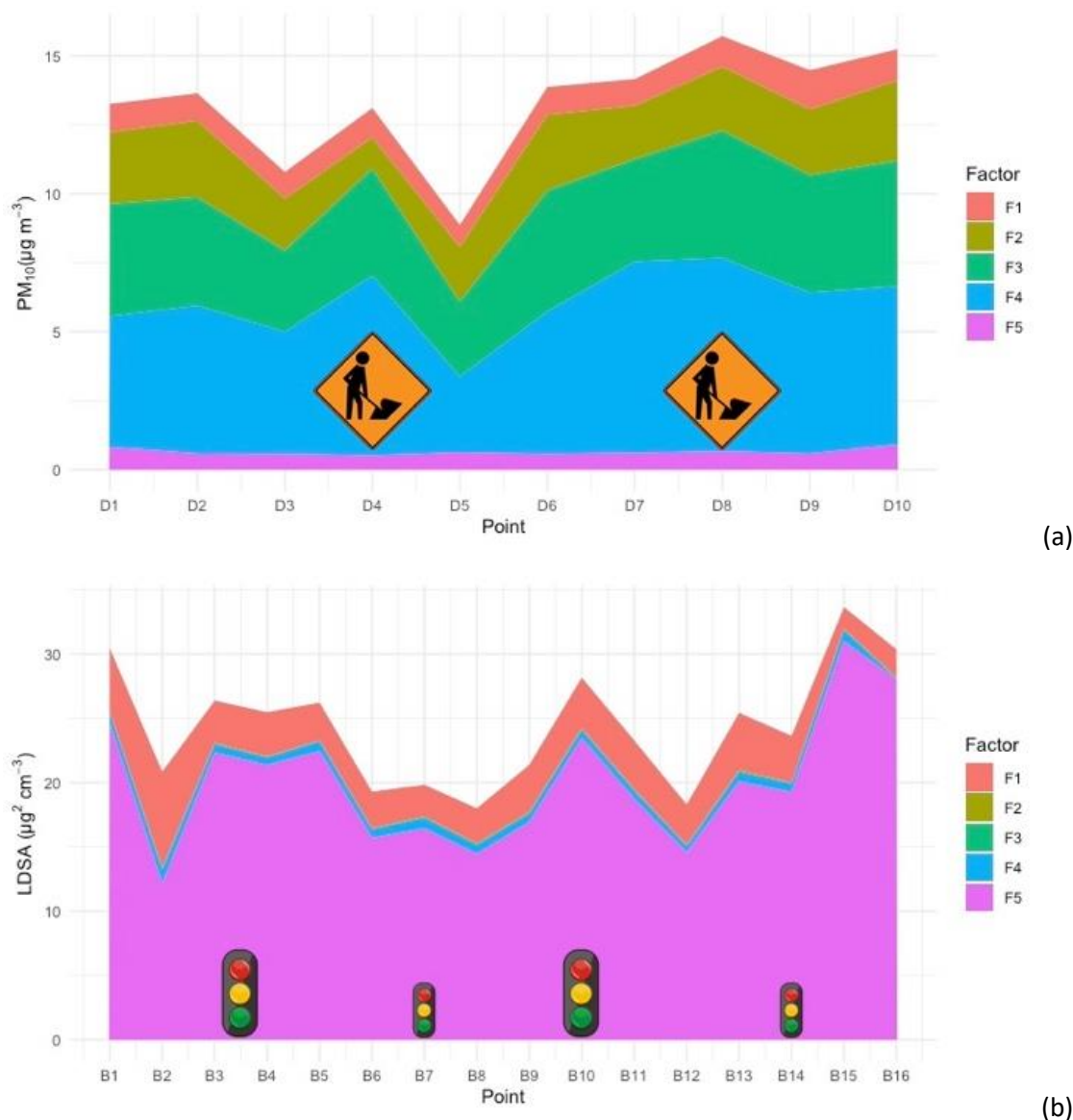


**Figure 4. (a)** Variation of the sources of PM<sub>10</sub> for a transect across Dawlish Road, a relatively small residential road. The location of construction sites is highlighted. **(b)** Variation of the sources of the LDSA for a transect across Bristol Road, a road with significant traffic activity. The location of major (on a junction) and minor (no junction) traffic light points are marked. In both cases, F1 represents the Urban Background source, F3 the Marine source, F5 the traffic source and F2, F4 local sources.

### 3.4 Predicting PM<sub>2.5</sub> concentrations

#### Monitoring

For this project a combination of the data collected from the aforementioned monitoring activities was used. Additionally, traffic count, topography and demographic data were used. These data were acquired either by the Birmingham City Council, or through internet repositories. As the data from multiple (total of 10) OPC-N3 were used, a collocation of these sensors would be a more appropriate calibration method. While these sensors measure very similarly between them, their performance against a single research grade instrument may vary. This is because LCS, while responding similarly to different meteorological conditions, the intensity of their effect on them may vary significantly. Thus, discrepancies and erroneous data may be observed. Data from multiple sources were

used as an input to different machine learning methodologies, with which we tried to predict PM concentrations and fill gaps when data was not available.

#### *Data processing*

For the calibration of the OPC-N3s in this case, though we had one-on-one data with them against the research grade instruments at the BAQS, a collocation and calibration of the OPC-N3 against each other, and then a calibration of one of them against the research grade instruments was found to have the best outcome.

The dataset in this case consisted of multiple different types of data which needed to be inputted to the machine learning methods. Data were combined and used in 10 seconds resolution. This was done to include detailed data from the mobile measurements.

For the training and testing of model performance we used the 80-20 approach. This meant that we used 80% of the data to train the model and 20% from PM for model evaluation. This was done in multiple repetitions using resampling to assure the uniformity and repeatability of the results.

#### *Results*

The results we got from the analysis of the data helps in creating a model which can be used to fill data gaps and predict PM concentrations when measured data is not available (Baruah et al., 2024). The analysis indicated that the models performed better when predicting PM<sub>2.5</sub> than PM<sub>10</sub>, data, which was more difficult to model (Figure 5). Communication and data acquisition from the Birmingham city council was easy. City councils are usually willing to provide data. Demographic data were acquired using open online repositories and were very helpful in developing the models.

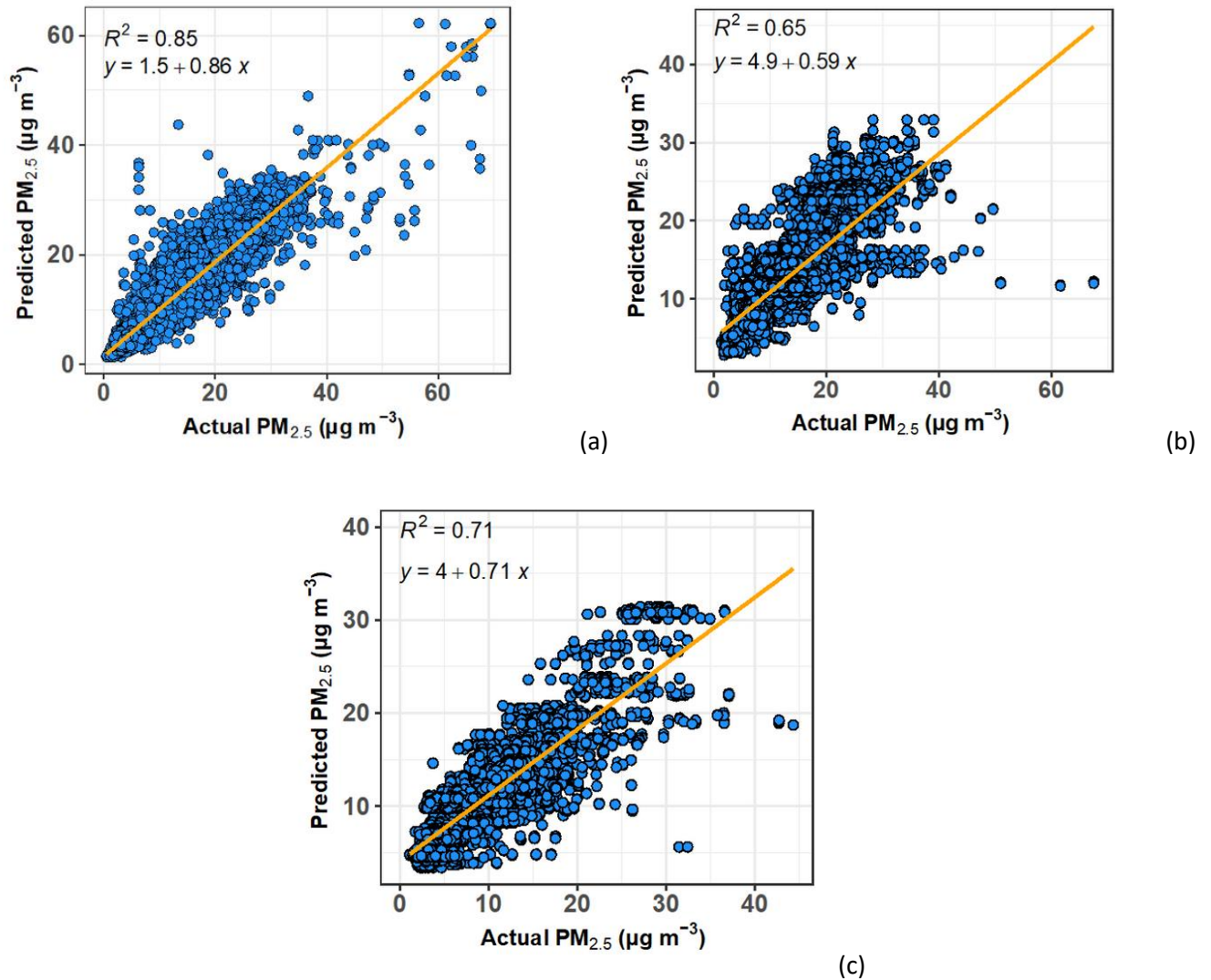


**Figure 5.** Linear regression between Actual and predicted  $PM_{2.5}$  concentrations for a) the Standard Random Forest Regression, b) the best Sensor Transferability Evaluation and c) for the Best Road Transferability.

### 3.5 Gaussian-based dispersion modelling approach with the ADMS-Urban model over Birmingham

The local scale ADMS-Urban Gaussian plume air dispersion model has been used for the Birmingham Pilot to generate high resolution air quality datasets for  $NO_2$ ,  $PM_{2.5}$  and PNC (Zhong et al., 2021; Zhong et al., 2023). Meteorological parameters measured at Birmingham Airport synoptic meteorological site were applied to drive the atmospheric dispersion in the boundary layer in the model. Background concentration input files were derived based on measured air quality datasets from rural background sites (available via the UK Automatic Urban and Rural Network, AURN) surrounding the West Midlands region. The upwind background site for each hour over the year was selected based on the monitored wind direction at that hour for  $NO_2$ , and  $PM_{2.5}$ . For PNC, there is a limited number of AURN sites in the UK, and Chilbolton was considered as an appropriate rural background site to inform the modelling background. For  $NO_2$  and  $PM_{2.5}$ , the emission inventories were derived based on the UK NAEI emissions at a spatial resolution of  $1\text{ km} \times 1\text{ km}$ . Unlike emission inventories for traditional air pollutants (e.g.  $NO_2$  and  $PM_{2.5}$ ), there are limited sources for the emission inventory for UFPs in the UK. Therefore, for particle number, the emission inventory developed in the RI-Urbans project with a  $6\text{ km} \times 6\text{ km}$  spatial resolution was taken as an

input for gridded emissions in the ADMS-Urban model. For the explicit major road emissions, the local traffic model datasets for traffic activities, average speed and fleet composition have been obtained from Transport for West Midlands and Birmingham City Council. An Atmospheric Emissions Inventory Toolkit (EMIT developed by Cambridge Environmental Research Consultants, CERC) has been used to pre-process all types of emission sources before these can be formatted and used by the ADMS-Urban model. The advanced street canyon and urban canopy modules have been applied to consider local street canyon effect on reduced dispersion of air pollutants and urban canopy effect on larger scale atmospheric flow due to spatially varying roughness length. A novel task farming approach was adopted to optimise the computing time via the parallel running of on multiple cores on supercomputer clusters at the University of Birmingham. Simulations were for June, July and August 2019 (summer), and January, February and December 2019 (winter).

The simulated concentrations for receptor locations are evaluated by comparison to measured concentrations obtained from UK AURN and the BAQS supersites. Five background and three traffic stations are available to evaluate NO<sub>2</sub>, four background and one traffic stations are available to evaluate PM<sub>2.5</sub>, and one background station is available to evaluate PNC. The modelled concentrations satisfy the strictest performance criteria for NO<sub>2</sub> and PM<sub>2.5</sub> at both background and traffic stations in winter and summer, and the less strict performance criteria for PNC at the background station. The mean NO<sub>2</sub> concentrations are lower than Paris, but higher than Athens: they range between 13 and 29 µg m<sup>-3</sup> for NO<sub>2</sub>. Average concentrations of between 7 and 14 µg m<sup>-3</sup> for PM<sub>2.5</sub> were lower than Paris and Athens (in summer), but equal to Athens in winter. The average PNC are at least 5 times lower than in Paris: the average ranges between 2,100 #particles cm<sup>-3</sup> and 2,900 #particles cm<sup>-3</sup>. Figure 6 shows the PNC map, illustrating the importance of major roads. More than two-fold variability of average PNC is present in the maps.

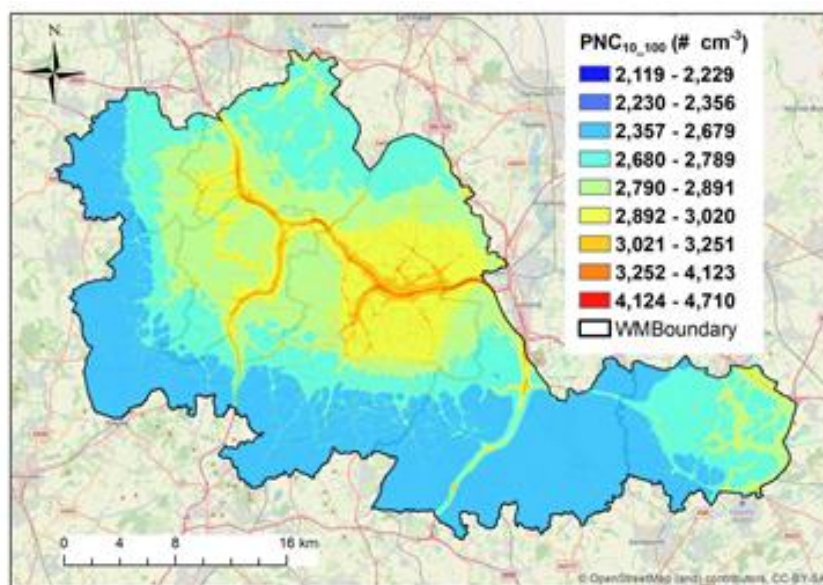


**Figure 6.** Average PNC in # of particles per cm<sup>3</sup> Birmingham, obtained by dispersion modeling.

## 4. ROTTERDAM: CITIZEN-BASED MOBILE MONITORING

Employees from the (1) city of Rotterdam and (2) DCMR conducted mobile monitoring following the airQmap (<https://airqmap.com/en>) procedure, with portable instruments for black carbon (BC) to map their exposure to BC and derive representative long-term average air quality maps during commuting hours. Monitoring campaigns were conducted in both winter season (2022) and summer season (2023) whilst cycling from and to work (typically during rush hour periods) with a combination of portable GPS and Micro Aethalometer AE51 (Aethlabs microAeth) instrumentation. Monitoring follows previously developed methods (van den Bossche, 2015). The campaign was coordinated by VITO in collaboration with DCMR and University of Utrecht. DCMR arranged the supervision of monitoring.

### 4.1. Monitoring strategy

Sampling was conducted whilst commuting and can, therefore, be regarded representative for commuting hours (rush hour periods; not constrained to 7-9h and 16-19h as can be seen on the temporal variability graph below), in both summer and winter season. The seasonal background concentration largely impacted the measured BC concentrations as can be seen on the figure below (Figure 7).

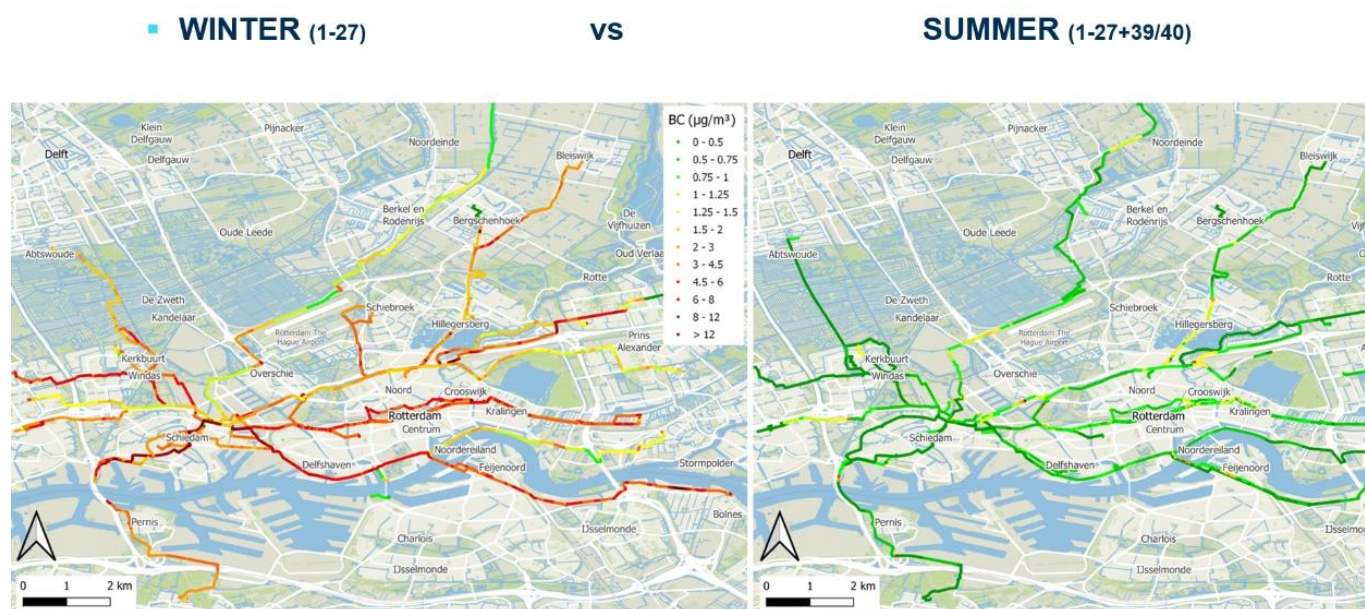


**Figure 7.** Average BC concentrations ( $\mu\text{g}/\text{m}^3$ ) derived from mobile monitoring involving citizens in the Rotterdam area.

### 4.2 Accuracy

The accuracy of the instruments was evaluated beforehand at VITO by means of a co-location campaign next to a reference instrument (Aethlabs, AE33 monitor). Inter-instrument variability is less than 10%. When comparing the temporal variability of the mobile BC data to the reference data that was available throughout Rotterdam, we observe similar hourly concentration variability as observed within the existing fixed site AQMN (Figure 8).

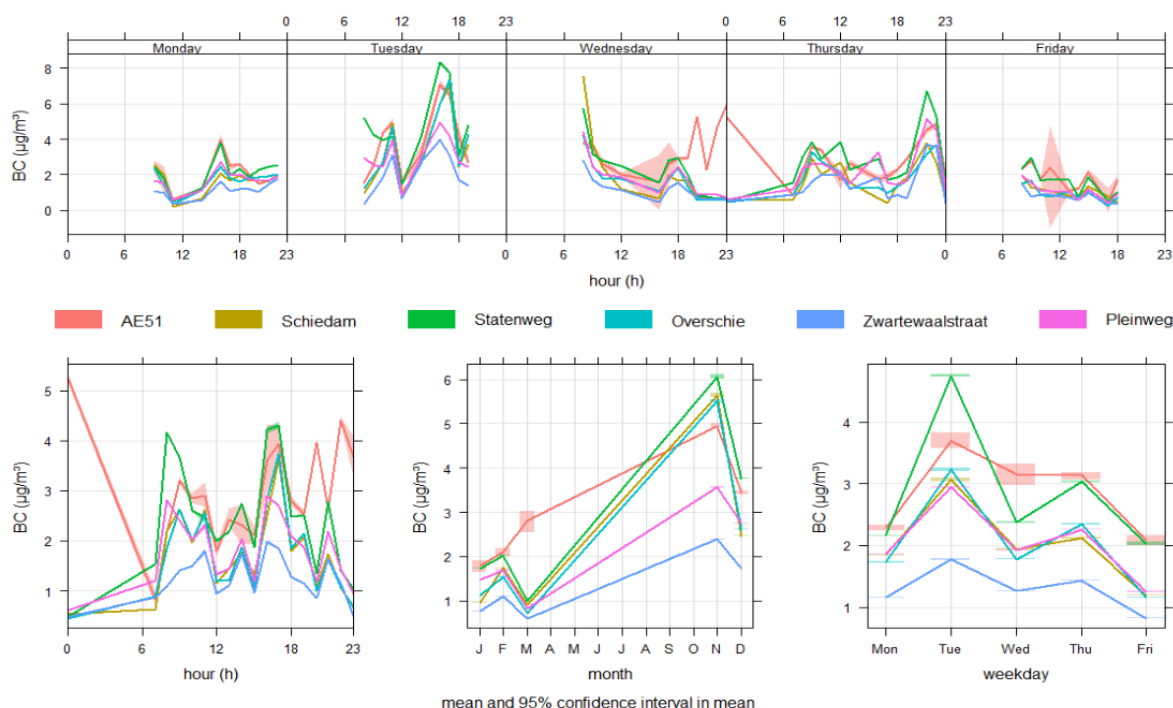


**Figure 8.** Diurnal variation of BC concentrations ( $\mu\text{g}/\text{m}^3$ ) derived from mobile monitoring (AE51) and routine monitoring stations (with AE33 instrument).

### 4.3 Normalization

Background normalization is necessary to interpret the measured concentration data, to correct for bias due to the fact that the sampling hours were during the morning and afternoon rush-hours. Use of reference monitoring data is essential to correct for sampling hour bias. We evaluated an additive or multiplicative normalization procedure of the point measurements, based on respective nearby urban background or roadside reference AQ monitoring stations (AQMS).

$$BC_{norm,i} = BC_i - BC_{bg,i} + \overline{BC}_{bg} \quad (\text{additive}) \quad (2a)$$

$$BC_{norm,i} = BC_i / BC_{bg,i} \cdot \overline{BC}_{bg} \quad (\text{multiplicative}) \quad (2b)$$

$BC_i$  = BC concentration from mobile monitoring time  $i$

$BC_{bg,i}$  = BC concentration from fixed background station time  $i$

$BC_{bg}$  = BC concentration from mobile monitoring time, average full study period

The additive normalization procedure was ultimately selected to normalize the collected mobile data and derive representative spatial maps of BC exposure. Based on the background normalization, maps could be derived showing hotspot locations (Figure 9):

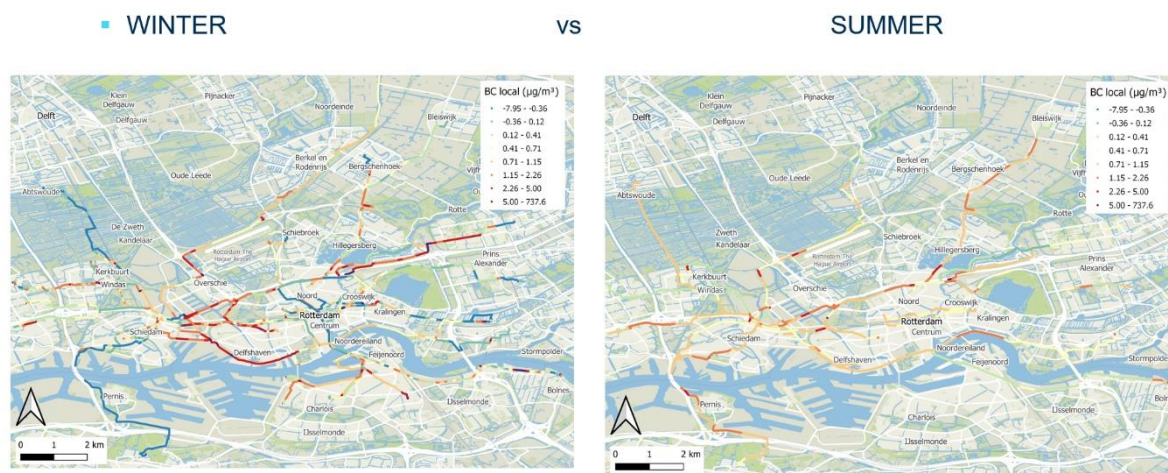


Figure 9. BC concentrations ( $\mu\text{g}/\text{m}^3$ ) derived from mobile monitoring by bicycle.

Locations with highest local contribution coincided with busy road traffic locations and/or cycling infrastructure in between road traffic.

#### 4.4 Number of repeats

The minimal number of required repeats for long-term average representativity, based on the subsampling analysis, varied between 24 and 54 (depending on the road segment) to be within 25% of the mean when considering the raw BC values, or between 22 and 39 when applying additional post-processing (winsorizing and/or background normalization).

## 5. ROTTERDAM CAR-BASED MOBILE MONITORING

### 5.1. Monitoring strategy

The aim was to produce long-term average air pollution concentration maps for the area, by the means of land use regression (LUR) models. A sub-question was to investigate if the industrial sources (mainly port activities) could be adequately captured in the mobile monitoring campaign.

We used a car to measure the ambient concentrations of  $\text{NO}_2$ , BC and UFP during two seasons in the city of Rotterdam; one campaign in November–December 2022 and another campaign in May–July 2023. The car was equipped with lab-grade 1 Hz  $\text{NO}_2$  (CAPS, Aerodyne Research Inc., USA), 1 Hz BC (AE33, Magee Scientific), and 1 Hz UFP (EPC 3783, TSI) monitors measuring simultaneously. A Global Positioning System (GPS) (G-Star IV, GlobalSat, Taiwan) was used to record the location of the car, which was linked to the measuring equipment via date and time. More details are provided in previous publications (Kerckhoffs, 2022). The measurements were mainly carried out between 8 to 22 hours every day in the study period (including some weekend days) in different parts of the city. The study area extended beyond the municipality of Rotterdam to cover sources in the area more broadly, include the harbour, industrial area, and airport. The “route” was discussed in detail with DCMR, the regional authority for the environment.

The study design was mostly a dedicated approach but it had elements of an opportunistic approach. The dedicated part comes from the fact that the area was divided into 8 polygons, each containing a part of the city center and residential areas as to randomize road characteristics at much as possible in each polygon (see Figure 10). Drivers



were instructed to drive in one polygon for each morning or afternoon session. Polygons were driven multiple times, each on a different day of the week and part of the day. The opportunistic part is that there were no specific routes that were followed. Drivers were asked to drive randomly on busy roads, residential roads and in industrial areas. Thus, the campaign does not rely on choices made by individuals for other reasons, such as the shortest route between home and work, as in the citizen-based campaign in section 4. This approach was chosen to reduce temporal dependencies in the data and limiting the need for temporal correction in the data processing. This is because all types of roads and corresponding co-variates were driven at different timepoints throughout the day and week, therefore, effectively reducing the correlation between the covariates and time of day.

Next to GPS systems in the car, all routes were tracked on a tablet visible by the driver as well. This app (MyTrack) enabled the drivers to see which streets were already driven, both in the current session and all previous measurement days.

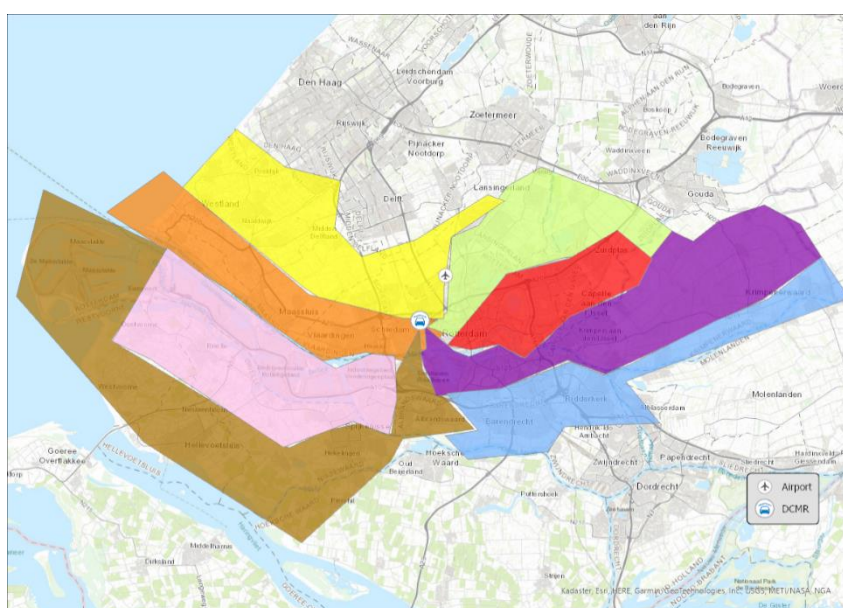


**Figure 10.** Overview of driving areas in the Rotterdam metropolitan area.

## 5.2 Number of repeats

The number of repetitions per location was low complicating measured data interpretation. The number of repetitions was low by design because the main purpose was to develop a model for which repetitions are not essential. Though winter and summer campaigns were used some bias arises from the fact that the driving was mainly on weekdays between 900h and 1900h. Our main goal was to create a LUR model based on all mobile monitoring, so repeats were not strictly necessary. Temporal and spatial variation in the data is more important. All topographies and road characteristics need to be monitored in the area (on different times of the week and day) in order to create robust models. Adding repeats increases the training performance of the model (because training instances are more accurate) but not the testing performance of the model.

The time resolution of all our instruments was 1Hz. Though only the UFP device was accurate enough on this time base that no post-processing was needed other than deleting unrealistic values below  $500 \text{ particles cm}^{-3}$  and above  $5000000 \text{ particles cm}^{-3}$ . For the BC and  $\text{NO}_2$  device the 1-sec resolution gave too much noise, so a moving average of 6 seconds and 3 seconds was used, respectively.

### 5.3 Validation

All instruments used are lab-grade and not easily portable. At least, a car is needed to make use of these instruments in a true mobile setup. Validation of the instruments was done before the campaign, once per year. The instruments are lab-grade reference equipment and do not need to calibrate in between the measurements. Colocation was therefore only done to check values, not calibrating. While colocation with reference measurements was done, but not checked thoroughly before starting the monitoring campaign, leading to unreliable NO<sub>2</sub> measurements in terms of absolute values in the winter campaign. On top of that, we also validated the UFP measurements by driving our measurements car right after another exactly the same measurement car (used in other projects). Results show that a moving platform can very accurately pick up UFP concentrations while driving (Figure 11). Despite this QA-QC, mobile measurements of NO<sub>2</sub> during the winter campaign were lower than during the summer campaign and substantially lower than measured at routine monitoring sites in Rotterdam. Additional QA-QC procedures are needed. To properly maintain data quality, longer co-location than the current set-up of 1 hour is useful, though logistically complicated. Immediate evaluation of the comparison results needs to be organized with the data owner of the reference station.

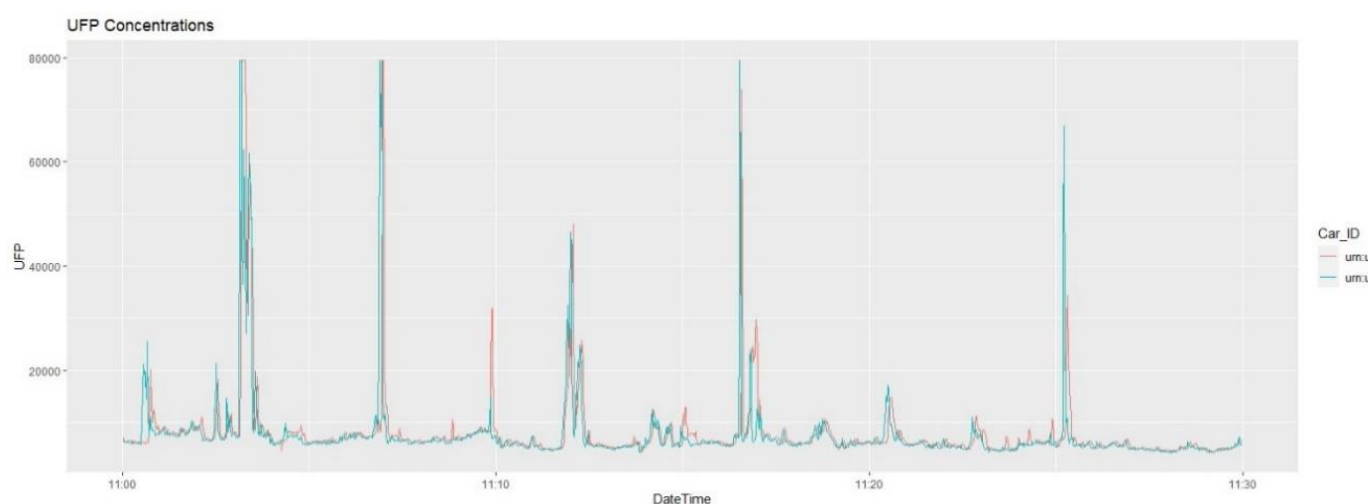


**Figure 11.** Example of UFP measurements (particles cm<sup>-3</sup>) on-board two cars during the Rotterdam pilot.

Since our aim was to create a model, we processed outliers by truncating them to the 5<sup>th</sup> and 95<sup>th</sup> percentile of the data. This means that very high or low values are not removed but remain very high (or low) without influencing the model too much.

### 5.4 Maps

The pilot was successful in producing plausible maps of the individual pollutants. The pilot was less successful when the interpretation rested upon monitoring data directly. The precision of the average concentration of our measurements per street segment is not high, since we measured most street segments only once or twice. As a data-only point this is far too little, but for creating a model this is not a limitation.

This pilot emphasized the seasonal (Table 1) and daytime difference of the pollutants. BC for example was very dependent on the season and meteorology in Rotterdam region, more than other cities measured so far. Though, models based on summer measurements were very similar to models based on winter measurements.

**Table 1.** Modelled concentrations of NO<sub>2</sub>, BC, PM<sub>2.5</sub>, and PNC in Rotterdam summer and winter.

	Concentrations ( $\mu\text{g m}^{-3}$ for NO <sub>2</sub> , BC and PM <sub>2.5</sub> and # particles cm <sup>-3</sup> for PNC)							
	NO <sub>2</sub>		BC		PM <sub>2.5</sub>		PNC	
	Mean	Min-max	Mean	Min-max	Mean	Min-max	Mean	Min-max
Summer	14.0	7 – 58	1.2	0.5 - 2.9	-	-	23,300	13,700-119,100
Winter	-	-	1.8	0.7 - 4.5	-	-	20,300	8,800 - 78,700

Mobile monitoring adds a lot of extra spatial variation in maps of air pollution, provided no high-resolution AQ modelling is available. Figures 12 – 14 document the maps for UFP, BC and NO<sub>2</sub>. Substantial variation related to various sources is observed, specifically traffic and port.

For UFP, currently not modelled and hardly monitored, the campaign did generate a lot of new/additional data and seemed to confirm new particle formation (NPF). However, due to the scarcity of repetitions the data is hard to compare to existing modeled data (unlike the cycling data). This also limits the interpretation of the new UFP data in relation to the well-established monitored and modeled data on other pollutants (e.g. BC, NO<sub>x</sub>, PM).

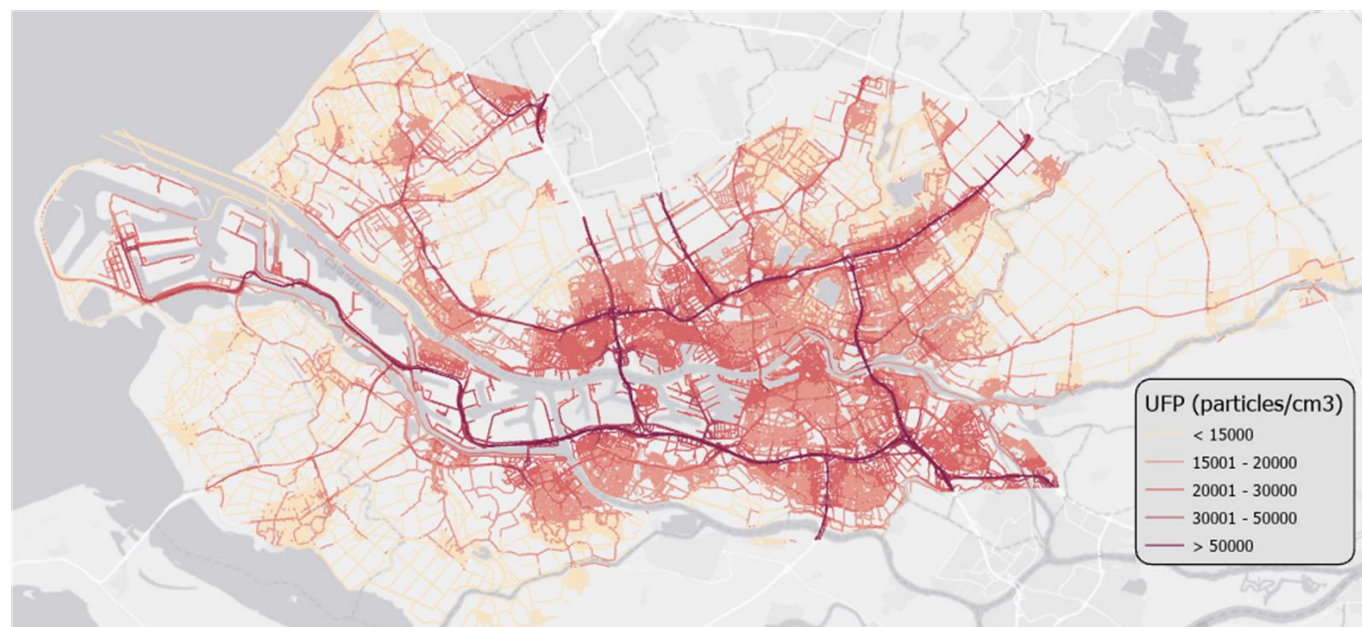


**Figure 12.** Mixed-effect model predictions for average UFP concentration levels in Rotterdam.

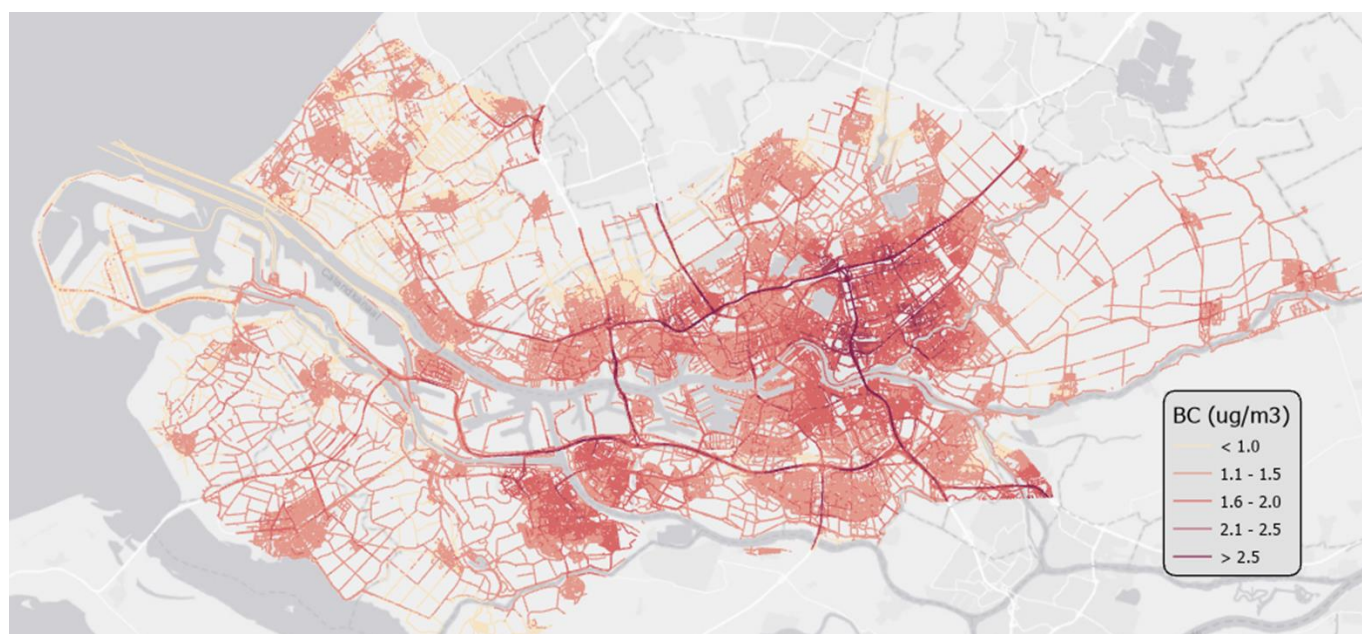


**Figure 13.** Mixed-effect model predictions for BC concentration levels in Rotterdam.

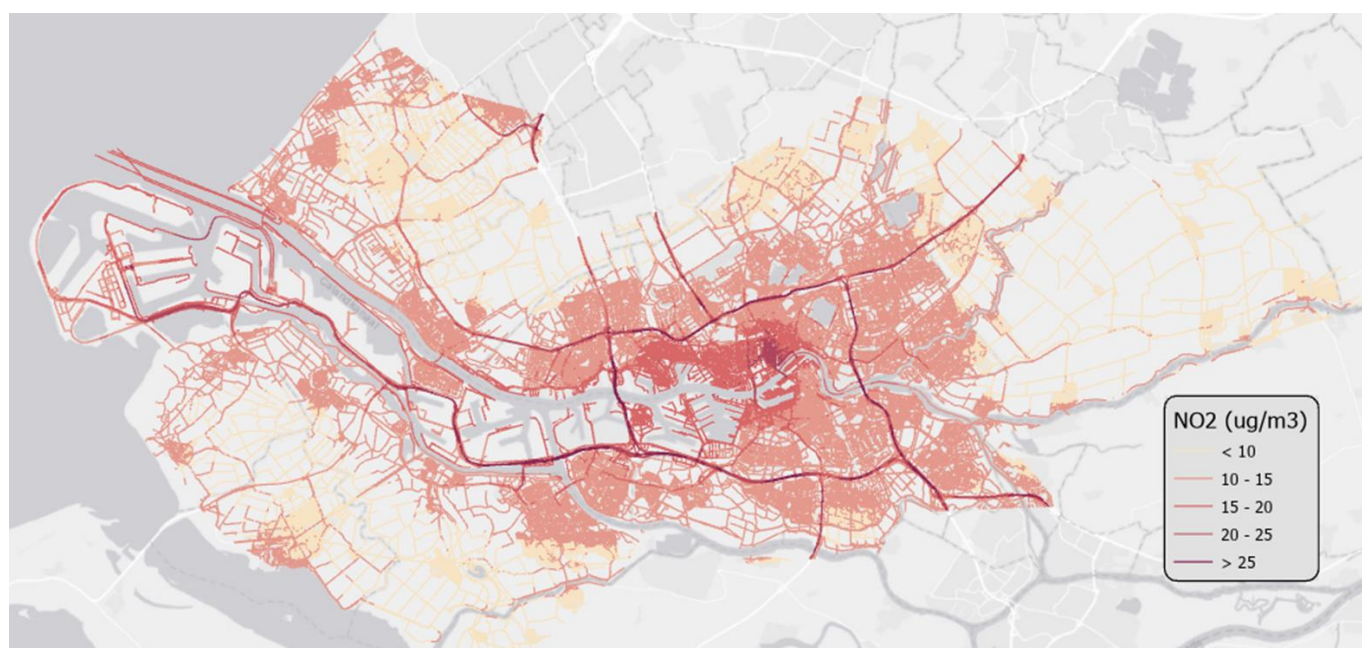


**Figure 14.** Mixed-effect model predictions for NO<sub>2</sub> concentration levels in Rotterdam.

The use of NO<sub>2</sub> rather than NO<sub>x</sub> was a good choice for health reasons and city LUR AQ mapping but for understanding air pollution mechanisms it is not useful. Normalizing UFP with NO<sub>x</sub> (to distinguish traffic and other sources) was not possible as NO<sub>2</sub>, especially in summer, is strongly impacted by photochemistry.

NFP was probably seen on summer afternoon. As UFP data are scarce in the Netherlands this is an important confirmation of this phenomenon in a rather 'northern town' albeit with many UFP precursors (seagoing ships, refineries, in addition to traffic).

We had hoped to compare UFP/BC or UFP/NO<sub>2</sub> ratios but due to data availability issues, including too few repetitions too small number of observations, it is hard to draw conclusions. With a systematic mobile monitoring in areas of interest, generating sufficient repetitions the mobile approach could have been more successful in mapping specific source areas. The ratios between the pollutants offer new insights into the source contribution of the pollutants. E.g. UFP is often elevated near airports, whereas BC and NO<sub>2</sub> are not. Similarly, one might expect to see areas with the influence of seagoing ships (supposedly the largest UFP source in the area), and the refineries. Figure 15 does seem to suggest some of the expected influences sporadically, while it shows unexpected results in others. The area near the airfield has similar colors as Barendrecht to the south of Rotterdam. From the map one could conclude either that there are two airports or that the info on the map is not indicative for an airport.

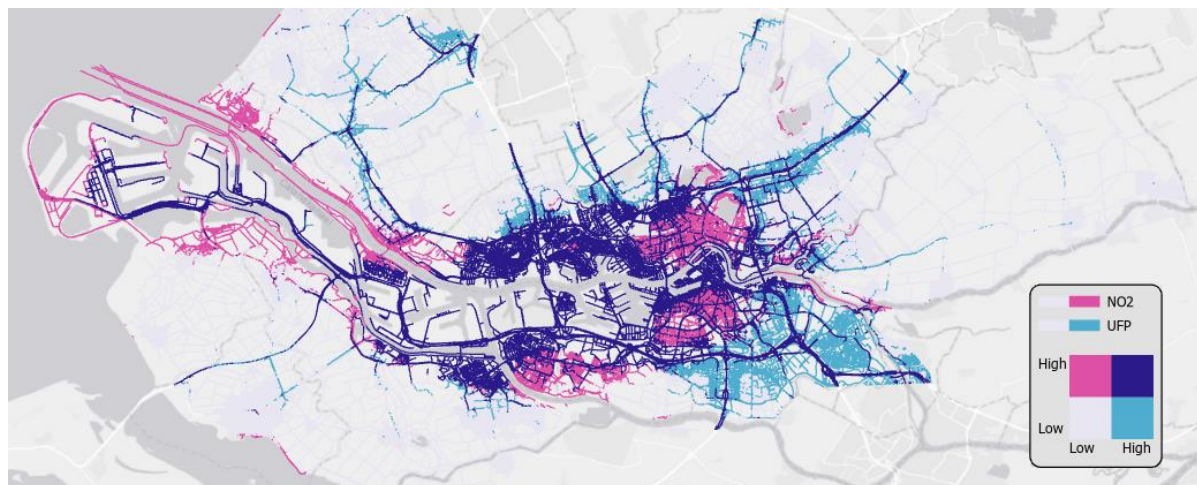


**Figure 15.** Ratio between predicted NO<sub>2</sub> and UFP concentrations in Rotterdam. Each of the four colors in the 2x2 box represent an equal number of road segments.

## 6. BUCHAREST PILOT

In the city of Bucharest summer and winter campaigns in 2022 and 2023, respectively, were carried out using mobile measurements without citizens' involvement. UFP, PM<sub>x</sub> and gaseous pollutants were measured. Moreover, the ESCAPE Land Use Regression models together with PyLUR tool and QGIS were implemented. Data analysis of the mobile campaigns, highlighting the summer and winter specific concentrations and distribution had been conducted.

### 6.1 Mobile measurements and data

Two mobile measurements campaigns representative for summer and winter periods have been conducted in Bucharest on 100 km route, with at least 15 repetition tracks per season. The route included heavy traffic roads inside the city, residential, industrial and commercial areas, as well as sub-urban areas. Portable instruments for UFP, different particle matter fractions (PM<sub>1</sub>, PM<sub>2.5</sub>, and M<sub>10</sub>) and gaseous compounds (NO<sub>2</sub>) have been used during both campaigns. The car measurements took place in the following timeframes: May – July (summer period, thereafter - summer) and January -February (winter period, thereafter - winter).

The measurements duration during one route were approximately 8 hours starting from 8:30 AM local time in order to capture data during rush hours, but also less intense traffic during the mid-day of working days. At least full 15 measurements routes were performed during each campaign, in different temperature conditions representative for the specific season.

## 6.2 Model

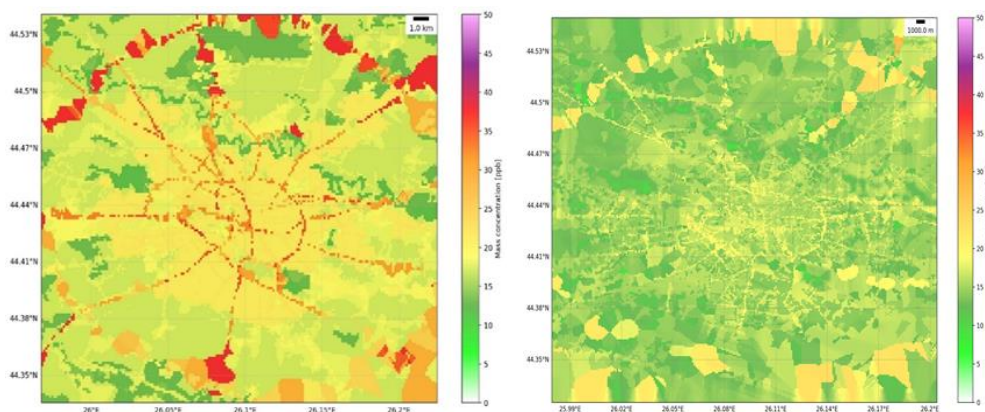
A Land Use Regression model, together with PyLUR tool and QGIS, was set up in order to create the pollutants maps during both seasons in the city of Bucharest. The goal is to create the air pollution maps for Bucharest area in order to assess the contribution of diverse area to air pollution, the gradients on particle concentrations between areas and related exposure along roads in different seasons or atmospheric conditions. A mixed effect model was also tested, using the mean value from the fixed effect model (LUR) together with the pollutant variability (intercept of mean standard deviation values) for all individual street segments at 1-minute intervals. Several LUR model configurations were established for each individual pollutant, the model with best hyperparameters (e.g.  $R^2$ , Root Mean Square Error, RMSE) being choose. Individual maps at 100 m grid have been retrieved for each season.

The model validation was carried out by comparison with standard measurements at selected fix reference sites from the National Air Quality Monitoring Network, while cross-validation was performed against in-situ data taken from the same collection.

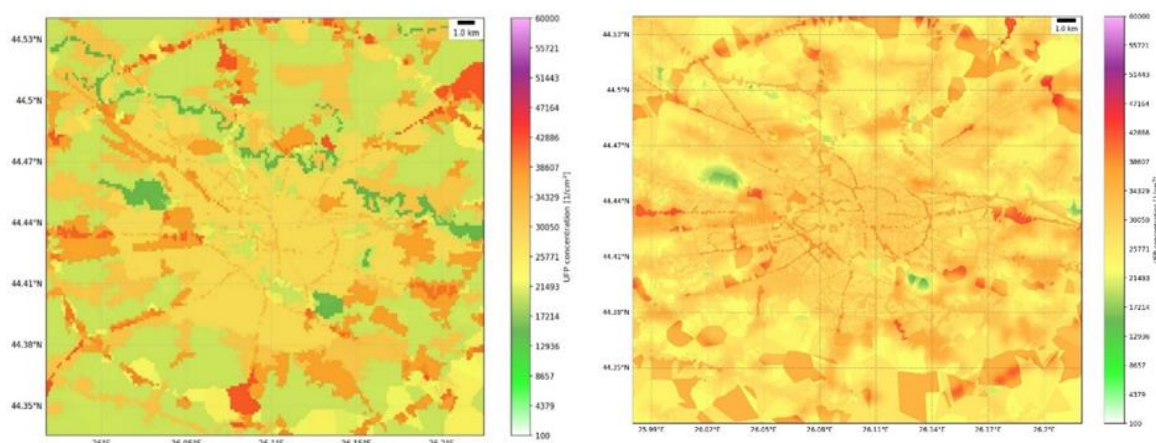
## 6.3 Maps based on car measurements

Figure 16 and Figure 17 represent maps of spatial variability for  $\text{NO}_2$ , and UFP in Bucharest during summer and winter periods, respectively. The UFP sources seem to be well distributed during summer period, while winter is characterized by more homogeneous sources. Significantly elevated concentrations are found mainly on the industrial area and urban agglomerations, but also on some important traffic routes. The average UFP number concentration along the mobile route presents a large spatial gradient mostly during summer, with differences up to a factor of 2 in the mean.

The  $\text{NO}_2$  concentration shows sharper gradients during summer, when the concentrations are higher on the main roads. On both seasons the main streets, including the Bucharest ring road, represents the main  $\text{NO}_2$  source. Also, the city center roads are highlighted, where the intensity of the traffic persists for the entire day. Seasonal variations of pollutants are also related to the height of the planetary boundary layer, linked to summer /winter.



**Figure 16.** Model maps for  $\text{NO}_2$  concentration levels in Bucharest during summer and winter period.



**Figure 17.** Model maps for UFP concentration levels in Bucharest during summer and winter period.

#### Evaluation of the summer and winter mapping by comparison to fixed measurements

The model performance has been evaluated for NO<sub>2</sub> and PM<sub>10</sub> concentrations using the hourly data available at the Romanian National Air Quality Monitoring Network (ANPM-8 fixed stations representative for urban, industrial and suburban areas) and at MARS supersite, which is part of RADO-Bucharest ACTRIS site (PM<sub>10</sub>/NO<sub>2</sub> for winter). Mean values of root mean square error (RMSE), Mean Fractional Bias (MFB) and Mean Fractional Error (MFE) are evaluated using the data from May-August 2022 and January-February 2023 (timeframe of the mobile measurements). Overall, the model performed well, NO<sub>2</sub> values are overestimated, while PM<sub>10</sub> levels are slightly underestimated (Table 2). As the model is trained with mobile on-road data, it is not surprising that it overestimates NO<sub>2</sub> exposures.

**Table 2.** Model performance metrics for NO<sub>2</sub> and PM<sub>10</sub> predicted concentration levels in Bucharest (Romania) during summer 2022 and winter 2023, when compared with measurements from fixed sites.

Pollutant	Season	Observed mean concentration	Modelled mean concentration
NO <sub>2</sub>	<i>summer</i>	12.58 ± 7.71 ppb	20.35 ± 0.70 ppb
	<i>winter</i>	15.98 ± 9.52 ppb	17.17±0.74 ppb
PM <sub>10</sub>	<i>summer</i>	24.64±13.18 µg/m <sup>3</sup>	22.94 ± 0.45 µg/m <sup>3</sup>
	<i>winter</i>	26.33 ±18.50µg/m <sup>3</sup>	27.81± 5.13 µg/m <sup>3</sup>

## 6.4 Variability within 1 km x 1km areas

Winter and summer maps for the normalised standard deviation (NSD) have been computed for all pollutants in order to assess the spatial sub-grid variability of concentrations within 1 km x 1 km areas (Figure 18 and Figure 19). A higher variability of pollutants concentrations is observed during the summer period, in the wintertime important variation are highlighted mostly on the ring road areas.

Similar variability patterns are observed for the particle's concentrations. UFP and NO<sub>2</sub> mean NSD are higher during summer.

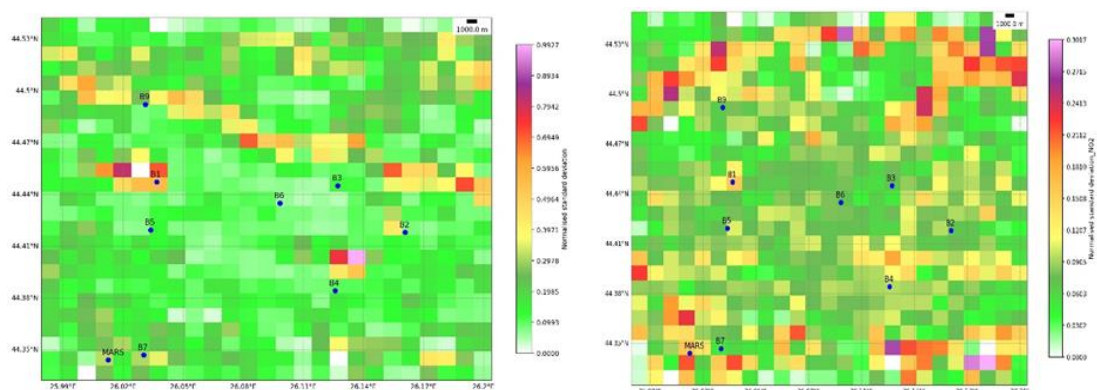


**Figure 18.** Normalised Standard Deviation of the sub-grids for NO<sub>2</sub> concentration levels in Bucharest during summer and winter period.

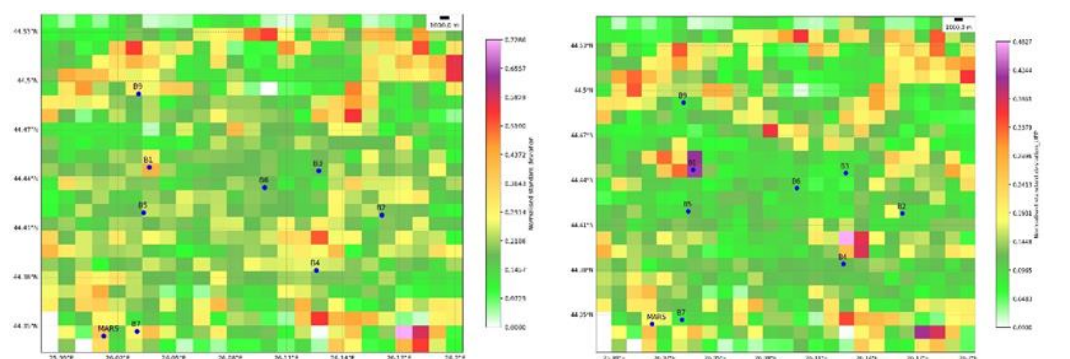


**Figure 19.** Normalised Standard Deviation of the sub-grids for UFP concentration levels in Bucharest during summer and winter period

## 6.5 Summary

This pilot highlights the seasonal difference of the pollutants corresponding to daytime working days. Both particulate matter and NO<sub>2</sub> concentrations were very dependent on the season and city area, being emphasized the industrial, residential or background areas. The main road areas present the highest concentrations of pollutants, both gases and particles concentrations having the highest concentrations on the West side of Bucharest.

The pilot campaigns and the model outputs extend the data available routinely for the Bucharest city both in time and space, fostering a better assessment of seasonal and spatial pollutants variability. Moreover, the pilot considers the UFP, which is not currently monitored, either modelled at the Bucharest level, in contrast to the standard



monitored particulate matter fractions or gaseous compounds. Therefore, the model output maps were validated only for PM<sub>10</sub> and NO<sub>2</sub> concentrations, due to the lack of other independent measurements for the rest of pollutants.

## 7. Paris pilot

Techniques based on deterministic modelling may also be used to provide high-resolution outdoor exposure city maps. They usually require an emission inventory, meteorological data and a model that estimates the evolution of concentrations in the atmosphere due to chemical and physical transformations. Background concentrations are calculated using the Eulerian chemical transport model CHIMERE (Menut et al. 2021). The simulated domain is discretized into cells of fixed size and the concentrations of the pollutants are assumed homogeneous in each grid cell. They typically have horizontal resolutions coarser than 1 km<sup>2</sup>. To represent the locally high concentrations, local-scale models represent the dispersion and sometimes the chemical transformation of the pollutants in the vicinity of their emissions. Two different approaches are used to represent the local dispersion over Paris: the Gaussian-based model ADMS (Stocker et al. 2012) and the street-network model MUNICH (Kim et al. 2022). The simulated concentrations may be corrected using data assimilation techniques and observations at fixed stations. Here, data assimilation is based on the BLUE (best linear unbiased estimator) algorithm of Tilloy et al. (2013).

Concentrations are measured and simulated over a winter and a summer period. The modelling set-up is briefly presented for each approach. Concentrations maps as well as model evaluation by comparisons to fixed measurement stations are also shown. For the comparisons to fixed measurement stations, hourly concentrations are evaluated by comparison to measurement stations using the Mean Fractional Bias (MFB), Mean Fractional Error (MFE), and the fraction 2 (FAC2), representing strict and less strict criteria for model evaluation (Boylan and Russell 2006, Hanna and Chang 2012).

### 7.1 Eulerian approach with the CHIMERE/MUNICH/SSH-aerosol chain over Paris

The Eulerian CHIMERE/MUNICH/SSH-aerosol chain was setup over Paris. The segments of the street network are those defined by Airparif, the Île-de-France air quality agency. They correspond to the main roads. The main street characteristics are obtained from the French BDTOPO database (<https://geoservices.ign.fr/bdtopo>). The street network is made of 4655 streets and extends over the city of Paris and its nearby suburbs. Regional-scale concentrations are simulated with the CHIMERE model (Menut et al. 2021) coupled to the street network MUNICH. The concentrations of NO<sub>2</sub>, PM<sub>2.5</sub>, UFP, BC and other particle components (e.g. inorganic and organic aerosols) are simulated. All the gas and particle components simulated at the regional scale are also simulated down to the street scale. Indeed, the chain CHIMERE/MUNICH use the same aerosol module (SSH-aerosol, Sartelet et al. 2020) at both the regional and local scales, allowing it to take into account the dynamic of particles at all scales. In the CHIMERE/MUNICH chain, nested domains are considered using CAMS boundary conditions over Europe. The smallest domain of CHIMERE simulation is discretized with a 1 km<sup>2</sup> resolution over Greater Paris. A zoom is performed in the streets of Paris, which are explicitly represented using a Eulerian approach with the street network MUNICH. The bottom-up Airparif inventory of the year 2019 is used, except for the traffic fleet and emissions which are specific to the period of simulation (winter 2020 and summer 2022 here). The road traffic emissions data were produced based on the results obtained using the Heaven system. The strength of this system is to use a traffic model that is corrected from the count data received in near real time. In the chain CHIMERE/MUNICH, the regional-scale traffic emissions were estimated by aggregating the local-scale emissions.

Number emissions and the size distribution of emissions were estimated from the emission inventory using the methodology detailed in Sartelet et al. (2022) and Park et al. (2024). The emission inventories provide estimations of PM<sub>2.5</sub> emissions for the different activity sectors. To distribute PM<sub>2.5</sub> emissions in the modelled particle size

sections, emissions of particles in the range  $PM_{0.1}$ - $PM_1$  and  $PM_{0.01}$ - $PM_{0.1}$  are estimated using the  $PM_1/PM_{2.5}$  and  $PM_{0.1}/PM_1$  ratios given in Sartelet et al. (2022) (Table A2) for each activity sector. The emissions in each of the size ranges:  $PM_{0.01}$ - $PM_{0.1}$ ,  $PM_{0.1}$ - $PM_1$ , and  $PM_1$ - $PM_{2.5}$  are then distributed amongst the model size sections with an algorithm that conserves mass and number. Note that for the residential sector, the lowest diameter considered for emission is 80 nm (against 10 nm for the other sectors).

For comparisons to observations, the simulated BC concentrations are obtained by multiplying the simulated EC concentrations by a harmonization factor, following Savadkoobi et al. (2024). A harmonization factor of 1.79 and 1.70 was determined for Paris in the summer 2022 and the winter 2020/2021 respectively using EC and eBC collocated measurements at Châtelet-les-Halles station, which is an urban background station operated by Airparif in the centre of Paris. The simulation was performed with the set-up detailed in Park et al. (2024) between 2 June 2022 and 31 July 2022 for the summer period, and between 7 December 2020 and 28 February 2021 for the winter period.

The simulated concentrations are evaluated by comparison to measurement stations from the Airparif network, as well as from a Airparif campaign for the winter period 2020/2021. Regional-scale concentrations (in 1 km<sup>2</sup> cells) are compared to measurements at background stations, and street concentrations (in the street cells) are compared to measurements at traffic stations. 24 and 9 background and traffic stations respectively are available to evaluate NO<sub>2</sub> in summer and winter. For PM<sub>2.5</sub>, 10 and 8 background stations are available in the summer and winter, and the number of traffic stations is lower: 3 and 1 in summer and winter. Less stations are available to evaluate BC: 4 background and 2 traffic stations in both winter and summer, while for UFP only background stations are available: 4 in the summer and 5 in the winter. The mean NO<sub>2</sub>, BC, PM<sub>2.5</sub> and UFP at urban background stations are higher than the concentrations at traffic sites. As detailed in Tables 3 to 6, the modelled concentrations satisfy the strictest performance criteria for all pollutants (NO<sub>2</sub>, BC, PM<sub>2.5</sub> and UFP) at both background and traffic stations. Maps of the concentrations are illustrated in Figures 20 and 21 for summer and winter respectively.

**Table 3.** NO<sub>2</sub> model to measurement comparisons at background and traffic stations for summer and winter in the Paris area (simulation with CHIMERE/MUNICH).

NO <sub>2</sub>	Station	Nb of Stations	Obs. (µg m <sup>-3</sup> )	Sim. (µg m <sup>-3</sup> )	MFE (%)	MFB (%)	FAC2 (%)
Summer	Background	24	15.0	14.5	32	-1	90
	Traffic	9	41.2	38.0	29	-1	94
Winter	Background	24	25.1	25.2	29	-3	93
	Traffic	9	43.4	52.1	28	19	96

**Table 4.** BC model to measurement comparisons at background and traffic stations for summer and winter in the Paris area (simulation with CHIMERE/MUNICH).

BC	Station	Nb of Stations	Obs. (µg m <sup>-3</sup> )	Sim. (µg m <sup>-3</sup> )	MFE (%)	MFB (%)	FAC2 (%)
Summer	Background	4	0.9	0.7	34	-19	86
	Traffic	2	2.8	2.6	33	3	91
Winter	Background	4	1.3	1.5	43	23	78
	Traffic	2	3.2	3.7	46	28	79

**Table 5.** *PM<sub>2.5</sub> model to measurement comparisons at background and traffic stations for summer and winter in the Paris area (simulation with CHIMERE/MUNICH).*

<i>PM<sub>2.5</sub></i>	Station	Nb of Stations	Obs. ( $\mu\text{g m}^{-3}$ )	Sim. ( $\mu\text{g m}^{-3}$ )	MFE (%)	MFB (%)	FAC2 (%)
Summer	Background	10	6.9	6.8	30	2	93
	Traffic	3	11.2	9.9	27	-10	95
Winter	Background	8	12.1	13.2	39	17	84
	Traffic	1	17.2	22.0	31	23	93

**Table 6.** *UFP model to measurement comparisons at background stations for summer and winter in the Paris area (simulation with CHIMERE/MUNICH).*

<i>UFP</i>	Station type	Nb of Stations	Obs. ( $\mu\text{g m}^{-3}$ )	Sim. ( $\mu\text{g m}^{-3}$ )	MFE (%)	MFB (%)	FAC2 (%)
Summer	Background	4	8176	8173	25	4	98
Winter	Background	5	7091	8025	35	15	87

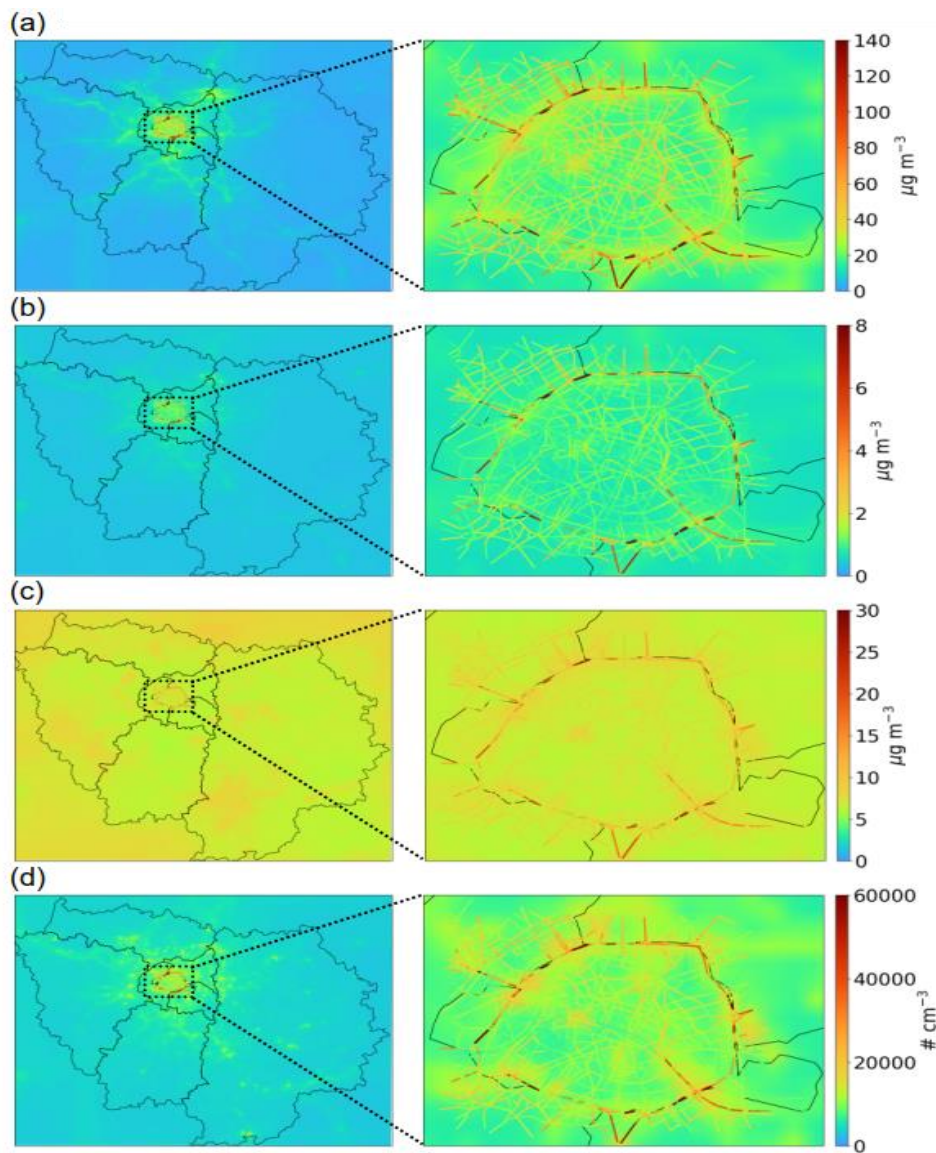


**Figure 20.**  $\text{NO}_2$  [panel (a)], BC [panel (b)],  $\text{PM}_{2.5}$  [panel (c)], and UFP [panel (d)] concentrations simulated for summer using CHIMERE/MUNICH.

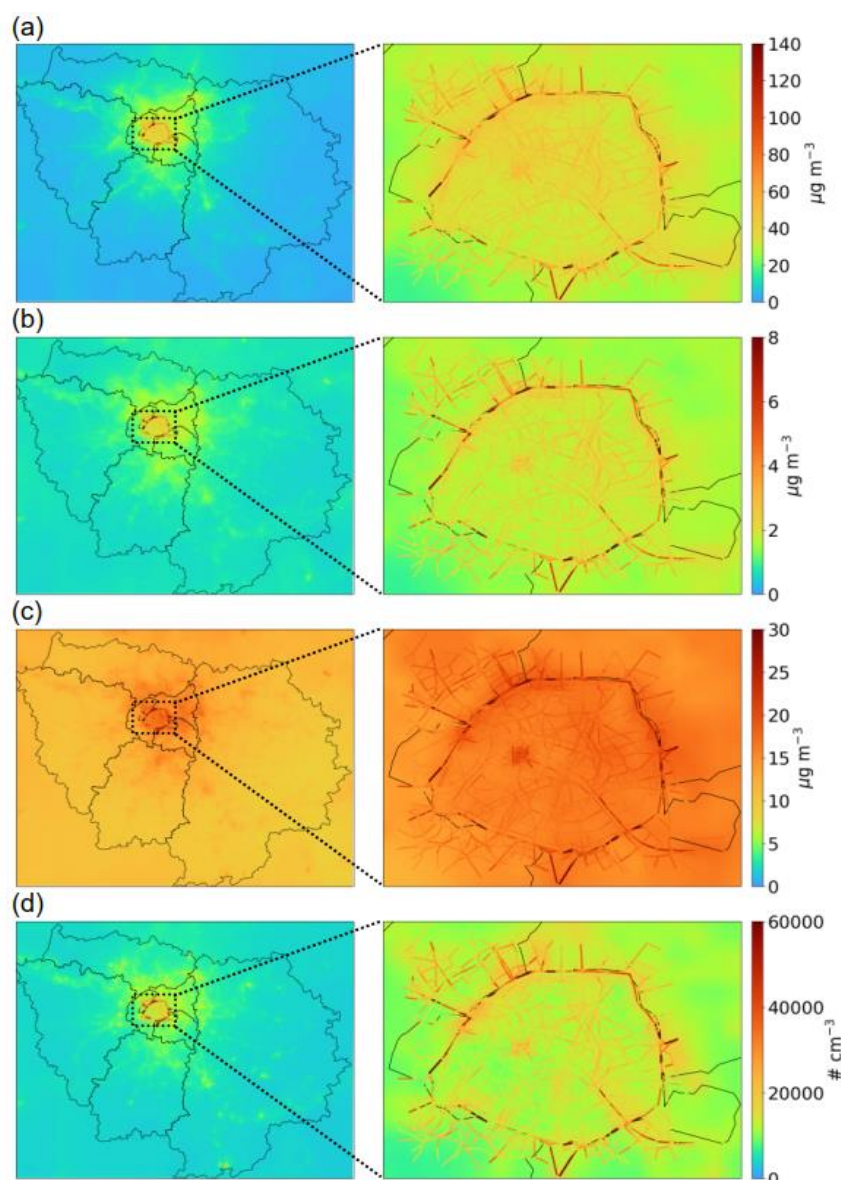


**Figure 21.**  $\text{NO}_2$  [panel (a)], BC [panel (b)],  $\text{PM}_{2.5}$  [panel (c)], and UFP [panel (d)] concentrations simulated for winter using CHIMERE/MUNICH.

## 7.2 Hybrid approach with the CHIMERE/ADMS chain over Paris

The Hybrid CHIMERE/ADMS chain was setup over Paris with and without data assimilation. The segments of the street network are the same as in section 3.1. Regional-scale concentrations are simulated with the CHIMERE model (Menut et al. 2021) at a 3 km x 3 km resolution, to which are superposed the local-scale concentrations simulated with the Gaussian-based model ADMS-Urban (Stocker et al. 2012). The concentrations of  $\text{NO}_2$ ,  $\text{PM}_{2.5}$  and BC are gridded at a 50 m x 50 m resolution. The boundary conditions of CHIMERE are obtained from CHIMERE simulations through PREV’AIR (<https://www.prevoir.org/>). The bottom-up Aiparif inventory is used, and at the local scale, traffic fleet and emissions are specific to the period of simulation as in 3.1. For comparisons to observations, the simulated BC concentrations are obtained by multiplying the simulated EC concentrations by a harmonization

factor, following Savadkoohi et al. (2024). The simulation was performed for June and July 2022 for the summer period, and January and February 2022 for the winter period. Although the summer period is the same as in the CHIMERE/MUNICH simulation, the winter period is a different year. It corresponds to the same year as the summer period (winter 2022), whereas winter 2020/2021 was chosen in the simulation with CHIMERE/MUNICH because of an intensive Airparif UFP measurement campaign that year. Maps of the concentrations are illustrated in Figures 22 to 25.

The simulated concentrations at a 50 m x 50 m resolution are evaluated by comparison to measurement stations from the Airparif network. As detailed in Tables 7 to 9, the modelled concentrations satisfy the strictest performance criteria for NO<sub>2</sub>, PM<sub>2.5</sub> and BC at background and traffic stations when data assimilation is not performed. NO<sub>2</sub> and BC concentrations are over-estimated at background sites, likely due to an overestimation of the background concentrations combined to the addition of both background and local contributions. Data assimilation systematically improves the error MFE and the FAC2 statistics. However, it sometimes leads to an increase in the bias MFB, especially at traffic stations for BC. This bias at traffic sites could be due to the limited number of stations at traffic sites for DA. Thus, the bias is higher for BC (only 2 to 3 traffic stations used for DA) than for NO<sub>2</sub> (9 stations used for DA). More observation stations would be needed for further improvements.

**Table 7.** NO<sub>2</sub> model to measurement comparisons at background and traffic stations for summer and winter in the Paris area (simulation with CHIMERE/ADMS).

NO <sub>2</sub>	Station		Nb of Stations	Obs. (µg m <sup>-3</sup> )	Sim. (µg m <sup>-3</sup> )	MFE (%)	MFB (%)	FAC2 (%)
Summer	Background	No Assimil.	24	15.0	19.8	41	24	80
		Assimilation			16.8	15	11	90
	Traffic	No Assimil.	9	41.2	37.8	30	-2	93
		Assimilation			34.1	19	-15	99
Winter	Background	No Assimil.	24	26.9	33.0	33	13	90
		Assimilation			28.4	9	7	100
	Traffic	No Assimil.	9	44.6	50.7	29	10	92
		Assimilation			40.8	12	-8	99

**Table 8.** BC model to measurement comparisons at background and traffic stations for summer and winter in the Paris area (simulation with CHIMERE/ADMS).

BC	Station		Nb of Stations	Obs. ( $\mu\text{g m}^{-3}$ )	Sim. ( $\mu\text{g m}^{-3}$ )	MFE (%)	MFB (%)	FAC2 (%)
Summer	Background	No Assimil.	4	0.86	1,0	43	17	76
		Assimilation			0.60	38	-34	91
	Traffic	No Assimil.	3	2.8	2.9	56	19	65
		Assimilation			2.7	15	1	100
Winter	Background	No Assimil.	4	1.4	1.2	43	23	65
		Assimilation			0.9	40	-34	87
	Traffic	No Assimil.	2	3.1	3.8	51	19	61
		Assimilation			2.7	19	-13	98

**Table 9.** PM<sub>2.5</sub> model to measurement comparisons at background and traffic stations for summer and winter in the Paris area (simulation with CHIMERE/ADMS).

PM <sub>2.5</sub>	Station		Nb of Stations	Obs. ( $\mu\text{g m}^{-3}$ )	Sim. ( $\mu\text{g m}^{-3}$ )	MFE (%)	MFB (%)	FAC2 (%)
Summer	Background	No Assimil.	10	6.9	6.6	26	0	95
		Assimilation			6.9	6	1	100
	Traffic	No Assimil.	3	11.2	11.6	21	3	98
		Assimilation			11.5	6	2	100
Winter	Background	No Assimil.	10	12.5	16.3	39	16	82
		Assimilation			12.4	6	0	100
	Traffic	No Assimil.	2	17.3	23.9	33	18	88
		Assimilation			17.0	6	-3	100

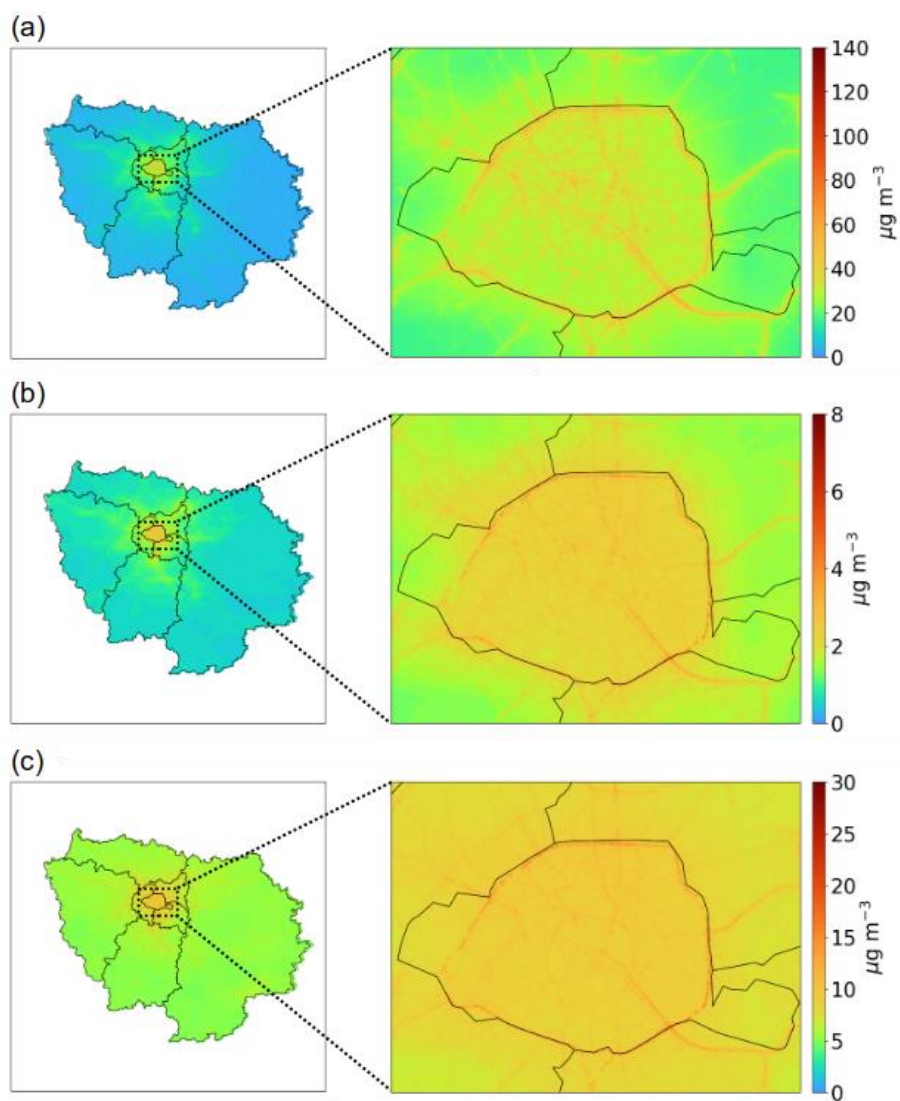


**Figure 22.**  $\text{NO}_2$  [panel (a)], BC [panel (b)],  $\text{PM}_{2.5}$  [panel (c)] concentrations simulated for summer using CHIMERE/ADMS.



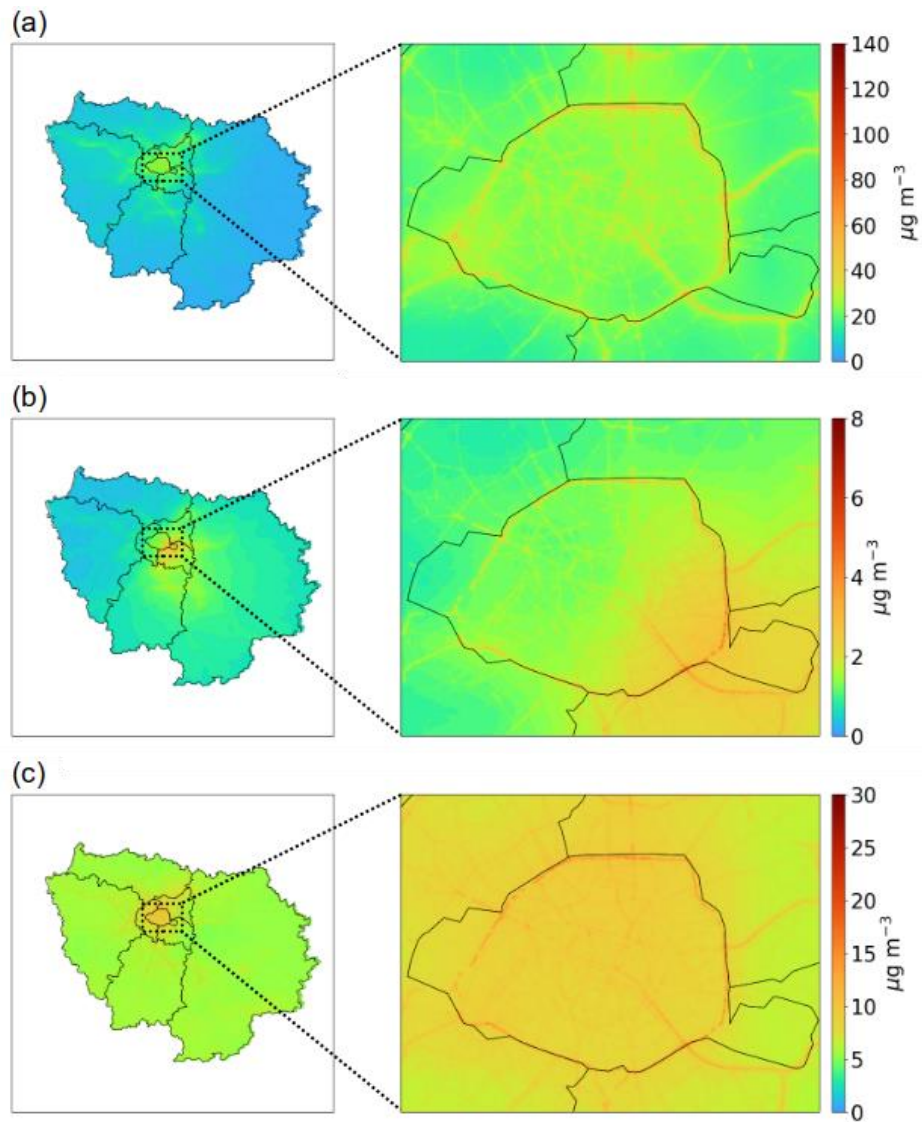


**Figure 23.**  $\text{NO}_2$  [panel (a)],  $\text{BC}$  [panel (b)],  $\text{PM}_{2.5}$  [panel (c)] concentrations simulated for summer using CHIMERE/ADMS assimilated.

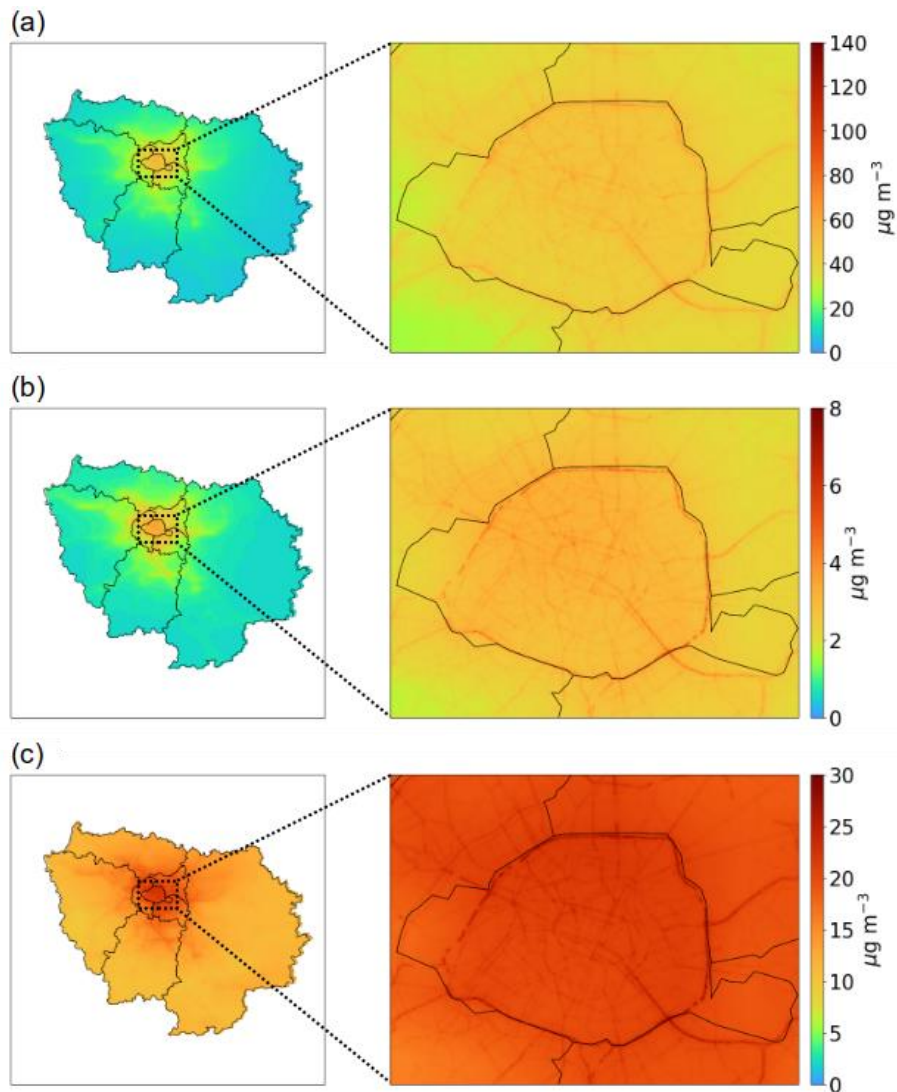


**Figure 24.**  $\text{NO}_2$  [panel (a)], BC [panel (b)] and  $\text{PM}_{2.5}$  [panel (c)] concentrations simulated for winter using CHIMERE/ADMS.

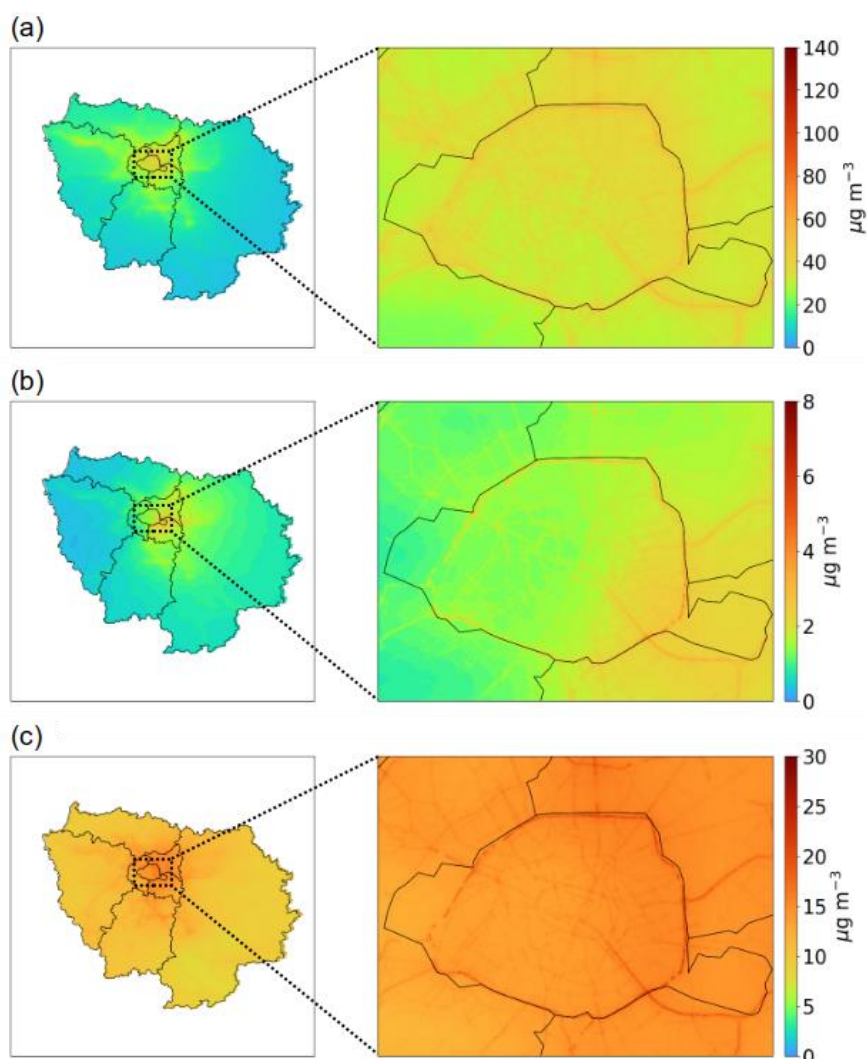


**Figure 25.**  $\text{NO}_2$  [panel (a)], BC [panel (b)], and  $\text{PM}_{2.5}$  [panel (c)] concentrations simulated for winter using CHIMERE/ADMS assimilated.

## 8. Athens Pilot

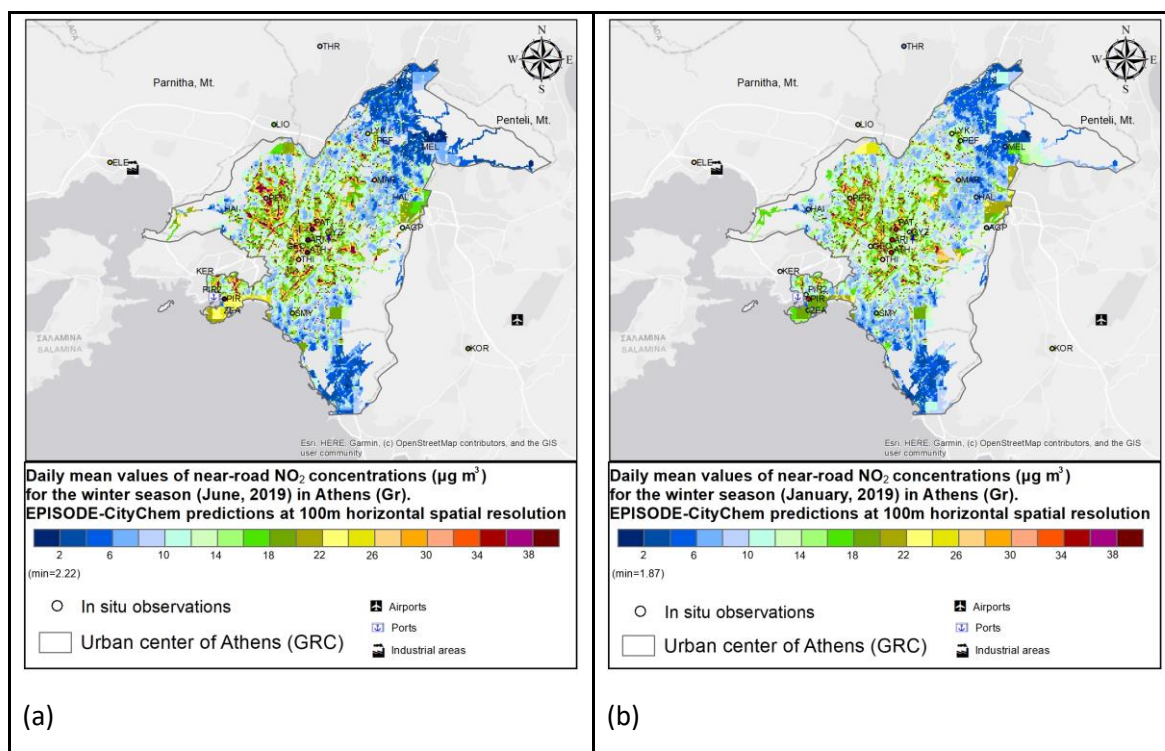
The concentration variability and outdoor population exposure to air pollution in Athens is assessed using the multi-scale numerical atmospheric model system CAMS/WRF/EPISODE-CityChem and the population data from the Global Human Settlement Layer (GHSL, <https://ghsl.jrc.ec.europa.eu/>). The core of the system is the chemistry transport model EPISODE-CityChem (Karl et al., 2019). Its comprehensive chemistry scheme is designed for treating complex atmospheric chemistry in urban areas and improved representation of the near-field dispersion. Input data (meteorology, boundary conditions, emissions) are heavily supported by Copernicus-related products. The model performs a specialized treatment on road and over the adjacent urban areas. Specifically, it is fed with hourly road network emissions in a linear format, applies a Gaussian dispersion scheme in the street canyons, and an extra photochemical scheme over the greater area of road surfaces, gridded in 100 m-by-100 m cells. These two schemes are superimposed to the Eulerian treatment of atmospheric processes in the whole 3D urban domain, with a horizontal spatial resolution of 1 km and a 24-layered atmosphere up to 3.7 km.

Local-scale atmospheric simulations are performed for 2019, which is a recent year, free of Covid-related activity restrictions, and with a wind field representative of 2016-2020. Numerical predictions have been evaluated against local air quality measurements from the National regulatory network and from the Panacea RI, using evaluation statistics, comparative time-series plots and selected outputs from the application of the benchmarking methodology developed in the framework of the Forum for Air Quality Modelling in Europe (FAIRMODE). Air quality maps at 1km and at 100m resolution are used to investigate spatial and temporal concentration variability.

### 8.1 Comparison of summer and winter concentrations

The month used to represent summer is July and for winter is January. Figure 26 shows the NO<sub>2</sub> and PM<sub>2.5</sub> high resolution (100m) concentrations for a mean day in summer and winter as predicted by EPISODE-CityChem. The concentrations of NO<sub>2</sub> tend to be higher along streets with high traffic in both seasons (Figures 26a and 26b). The spatial distribution of both pollutants is similar with higher NO<sub>2</sub> than PM<sub>2.5</sub> values at the inner-city center. The concentrations are higher in winter than in summer, especially for PM<sub>2.5</sub> (and for background NO<sub>2</sub>). The contributions of residential emissions from heating tend to increase particle concentrations during wintertime. NO<sub>2</sub> photochemistry is enhanced in Athens during summer-time, which is partly the reason for higher NO<sub>2</sub> concentrations at the traffic sites. Other reasons for seasonal differences include the lower boundary layer during wintertime and the stronger dispersion phenomena during summertime (incl. Etesian winds), which affect concentrations, mainly downwind the road network.

The simulated concentrations (in 100m cells) are evaluated by comparison to measurement stations using statistics such as Mean Fractional Bias (MFB), Mean Fractional Error (MFE), and root-mean-square error (RMSE) in Tables 10 and 11. For the 2 pollutants and station types, the mean concentrations compare well to the observations satisfying the model performance criteria (MFE < 75%, MFB < ±50%) and the model performance goal (MFE < 50% and MFB < ±30%) of Boylan and Russell (2006) in most cases.



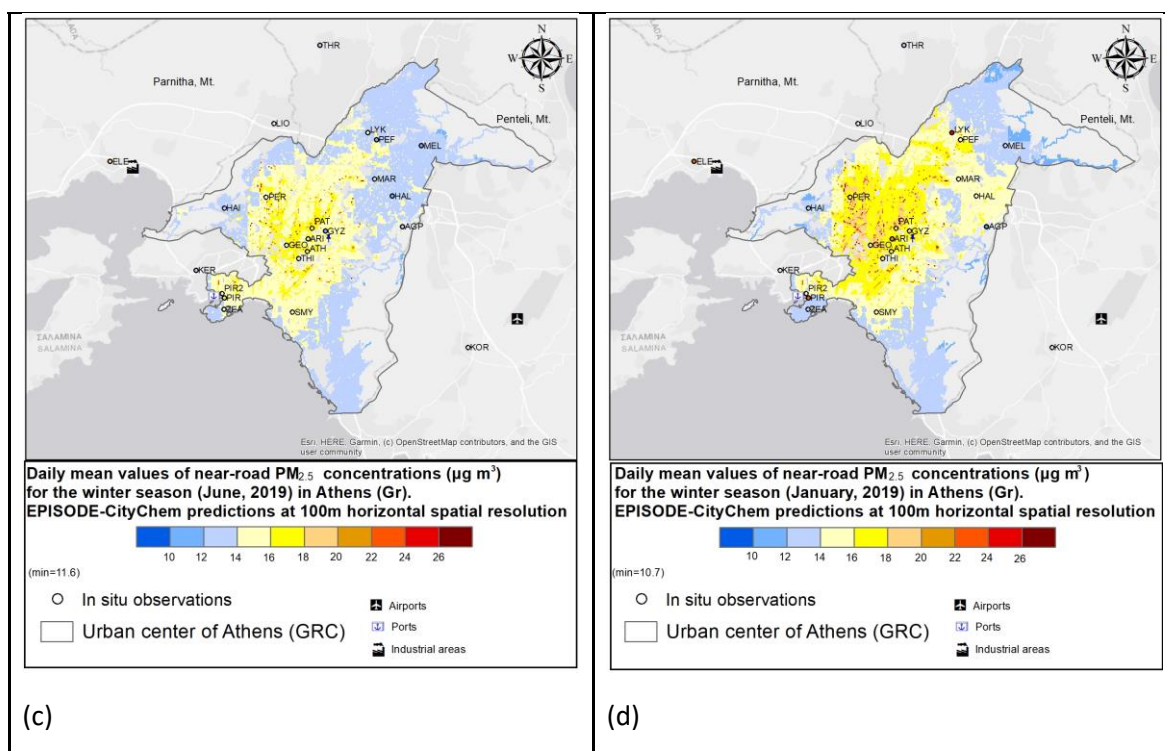


**Figure 26.**  $\text{NO}_2$  [(a) and (b)],  $\text{PM}_{2.5}$  [(c) and (d)], near-road concentrations ( $\mu\text{g m}^{-3}$ ) over Athens simulated for summer (left panels) and winter (right panels) using EPISODE-CityChem.

**Table 10.** NO<sub>2</sub> model to measurement comparisons at (urban) background and (traffic) roadside stations in Athens for summer and winter.

NO <sub>2</sub>	station type	No of stations/pairs	Obs. (µg m <sup>-3</sup> )	Sim. (µg m <sup>-3</sup> )	MFE (%)	MFB (%)	RMSE (µg m <sup>-3</sup> )	FAC2 (%)
summer	Urban	4/ 2747	19.5	13.5	22	-9	22.6	40
	Traffic	4/ 2964	59.6	44.0	24	-9	46.1	50
winter	Urban	4/ 2292	26.0	14.3	95	-72	23.1	35
	Traffic	4/ 2555	51.6	41.4	41	-11	34.2	59

**Table 11.** PM<sub>2.5</sub> model to measurement comparisons at (urban) background and (traffic) roadside stations in Athens for summer and winter.

PM <sub>2.5</sub>	station type	No of stations/pairs	Obs. (µg m <sup>-3</sup> )	Sim. (µg m <sup>-3</sup> )	MFE (%)	MFB (%)	RMSE (µg m <sup>-3</sup> )	FAC2 (%)
summer	Urban	1/ 699	12.6	15.3	30	20	5.8	96
	Traffic	2/ 1476	15.0	15.1	9	0	6.5	94
winter	-							
	Traffic	2/ 1438	23.1	17.6	67	-30	23.5	72

## 9. Helsinki pilots

In the context of RI-URBANS pilots regarding air quality variability in the Helsinki region, we performed a suite of intensive campaigns (Table 12). The work contributed to Task 4.3 on air quality mapping as well as to Task 4.5 with respect to the analysis of air quality hot-spots in urban environment. A brief summary of all campaigns, their location, targeted objectives, instrumentation, timing and reference providing additional information is provided in Table 12. The measurements for the campaigns are described in more detail in the sections below. In this deliverable we summarize the Kumpula BC mapping campaign results (Elomaa et al. 2024) and mobile bike-measurement campaign (Kleemola et al. 2024).

The RI-URBANS pilot activities in Helsinki took advantage of high-quality air quality observations in the Helsinki metropolitan area, specifically Mäkelänkatu supersite in the urban street canyon (Barreira et al., 2021) and Station for Measuring Earth-surface - Atmosphere Relations (SMEAR III, Järvi et al. 2006) in urban background environment in Kumpula Science Campus. These observation sites offer reference measurements for different air quality sensors and mobile measurements that allow spatial scaling of air quality. Such a hierarchical observation network was promoted by Hari et al. (2016) for climate research and by Kuula et al. (2021) for air quality applications.

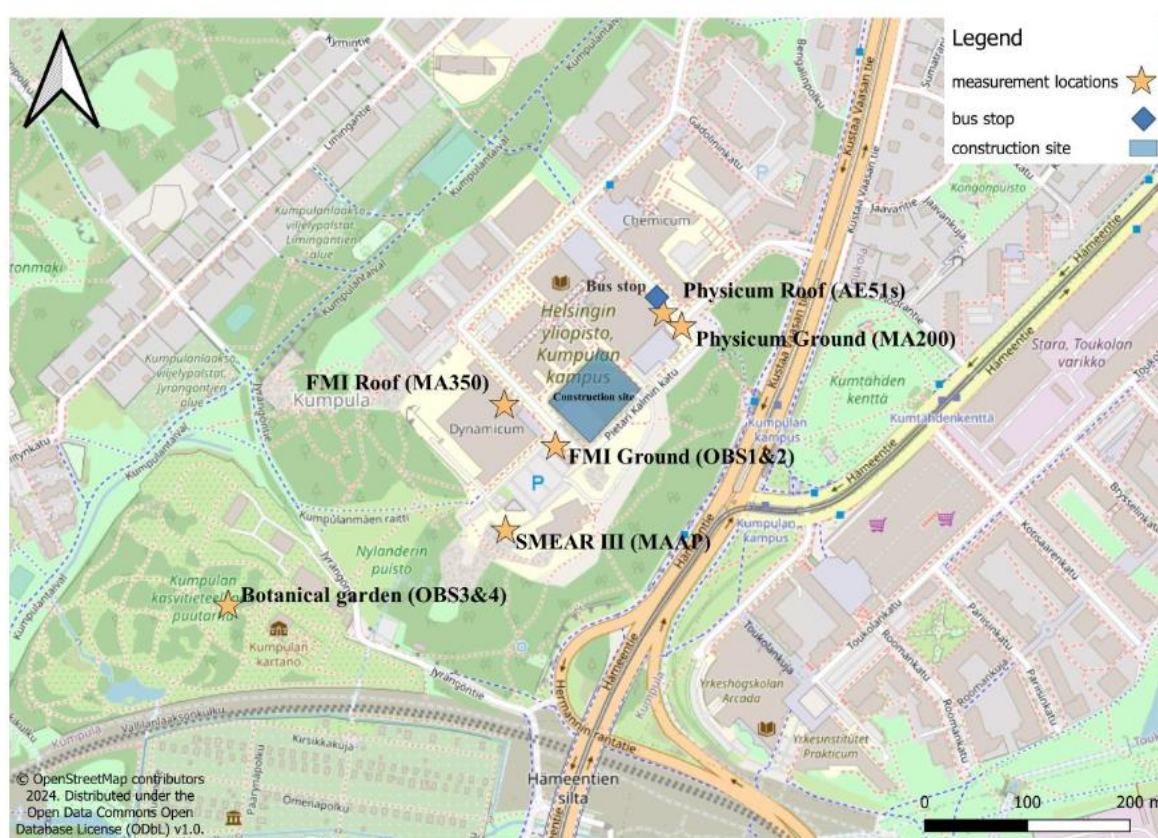
**Table 12.** Summary of RI-URBANS mapping and hot-spot campaigns in Helsinki.

Name of the campaign	Objective	Time	Instruments	Reference
Winter campaign (Task 4.5)	to quantify the role of wintertime conditions in aerosol and emission sources in urban environment	January-February, 2022	supersites + mobile lab	Teinilä et al. (2024)
Kumpula BC campaign (Task 4.3)	to quantify performance of small BC sensors against supersite observations; to quantify small scale variability of BC in urban background environment	summer 2021	BC sensors, MAAP	Elomaa et al. (2024)
Turunväylä campaign (Task 4.5)	to quantify the gradient of different air quality parameters as a function of distance from a highway	winter-spring-summer 2023	BC sensors, AQ-sensors, CPCs, lidar, mobile laboratory, drones, air quality modeling	Harni et al., manuscript under preparation
Bike-campaign	to quantify variability of air quality and particularly number concentrations in urban environment	summer 2024	CPCs, BC-sensors, meteorology	Kleemola et al. (2024)

(Task 4.3)				
------------	--	--	--	--

### 9.1 Kumpula BC-sensor campaign

During summer 2021 we deployed a network of four types of small-scale filter-based BC sensors (AE51, MA200, MA350, Observair) with the objective to evaluate these sensors for monitoring ambient BC concentrations and to study variations in high resolution. The observation network is presented in **Figure 27**. Prior and after the deployment, the sensor data was quality controlled against a reference BC instrument at SMEAR III observation site at the Kumpula Science Campus. The intercomparison measurements were conducted during 26.5. – 6.6. 2022 (11 d) and 16.9. – 3.10. 2022 (17 d). The intercomparisons showed comparable results for sensors and MAAP, thus validating the comparison.



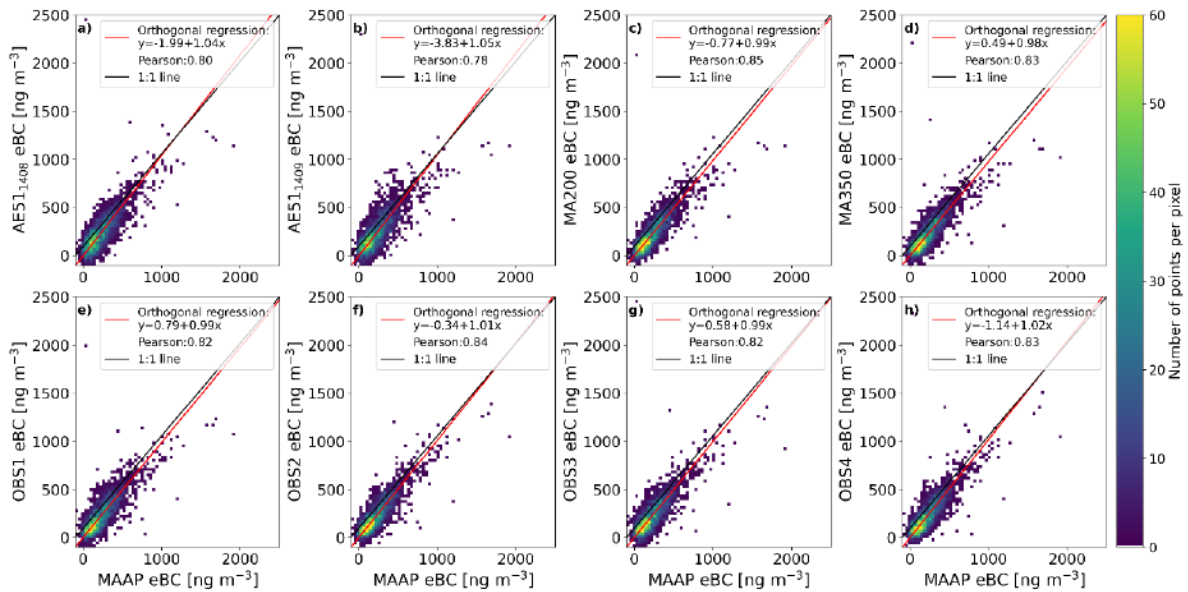
**Figure 27.** The locations of the BC sensors and SMEAR-III station. From Elomaa, T., et al. (2024).

Figure 28 shows the final result of the performance of the sensors after quality control against the BC reference. During the intercomparison period (26.5.-6.6.2022) the BC concentration reached occasionally concentrations up to 2000 ng m<sup>-3</sup> while during the majority of the time the concentrations remained from 100 ng m<sup>-3</sup> to 800 ng m<sup>-3</sup>. The sensor data correlated relatively well against the reference and the Pearson correlation coefficient varied from 0.78 – 0.84 with a slope from 0.84 – 1.13. After an orthogonal regression, the slopes converged into a range from 0.98 to 1.05.

The measurement campaign extended from June 2022 to September 2022 and after operating the instruments as a measurement network (Figure 27), the instruments were brought back into the supersite for the second



intercomparison. The agreement with the reference instrument remained at the same level. See Elomaa et al. (2024) for details.



**Figure 28.** Scattering of the BC data from different sensors against the reference instrument during the intercomparison campaign at SMEAR III (from Elomaa et al. 2024).

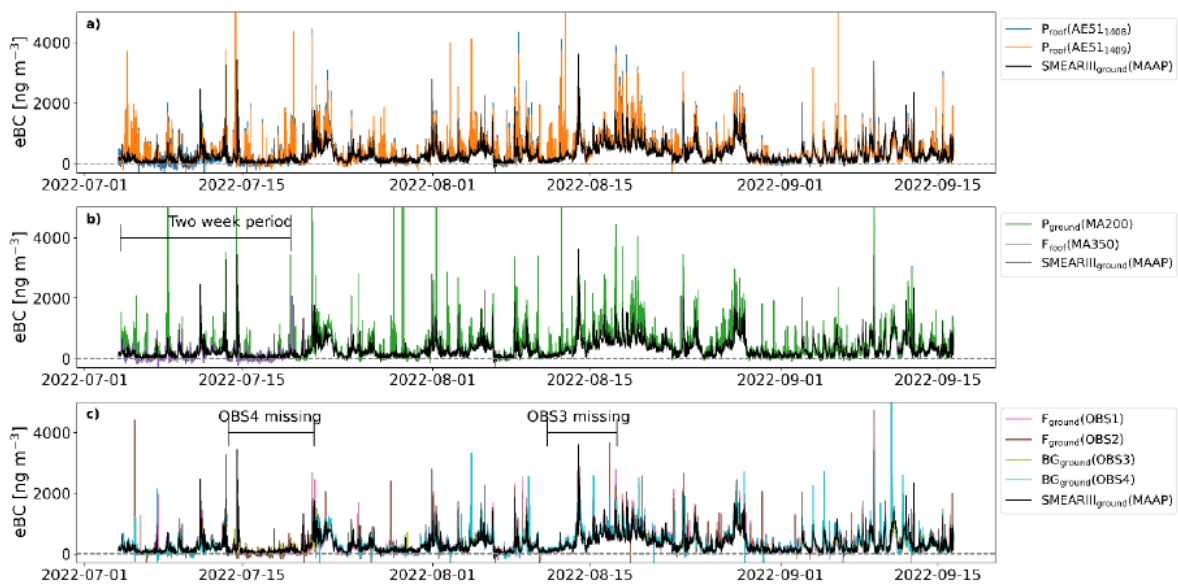


**Figure 29.** Time series of eBC data from the Kumpula Campus area with BC sensors in the locations indicated in Figure 27. Time period from 4.7.-16.9. is shown. From Elomaa et al. (2024).

Figure 29 provides the time series of the BC derived from the sensors. Sporadic and transient high values were observed both with sensors and with the reference instruments indicating spatially and temporally varying BC

sources in the area. Particularly for the sensors in the Physicum building ( $P_{\text{ground}}$  and  $P_{\text{roof}}$ ) were influenced by bus traffic between the Campus buildings. Approximately 160 buses per day transverse the campus area.

Figure 30 shows a wind-rose figure for the different BC sensors. The highest concentrations are associated with emissions from local traffic and the signature of the arterial road from Helsinki city center to Lahti (Kustaa Vaasantie in South East direction) provide a significant contribution to the observed BC concentrations. The local emissions from the traffic in the campus, including the city buses are clearly indicated by the wind-rose. The highest concentrations are in the ground level and roof level near the Physicum building and lower concentrations prevail further away from the bus lines ( $F_{\text{ground}}$  and SMEAR III).

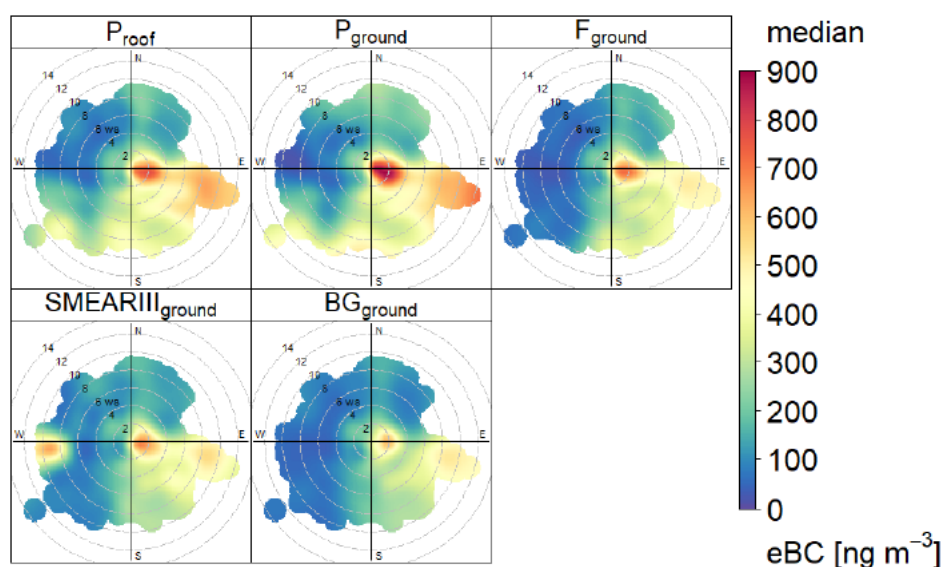


**Figure 30.** Equivalent BC concentrations at different measurement locations in Kumpula Campus area as a function of wind direction and wind speed. From Elomaa et al. (2024).

## 9.2 Bike campaign

As part of the pilot on air pollution mapping of the emerging air pollutants, we performed mobile measurements in Helsinki. The instrumentation were constructed on a bike (Figure 31) connected to cloud-services for data access.

The instrumentation on the bike included a battery-powered prototype Condensation Particle Counter (CPC) with laminar flow sampling. The working fluid was ethylene glycol. We included meteorological measurements, black carbon concentrations and optical counter for indicative PM<sub>2.5</sub> measurements.

With the bike we performed opportunistic sampling in the Helsinki region during June-September, 2024 on a route that connected areas with high variability in aerosol number concentration and two air quality supersites, namely SMEAR III (Järvi et al. 2006) in the Kumpula Campus area, and Mäkelänkatu supersite (Barreira et al., 2021) in the street canyon environment. Figure 32 shows a short intercomparison exercise (5 min co-location) done during the opportunistic sampling. The correlation is modest with a slope of 0.97. A more extensive intercomparison with exactly the same sampling conditions and longer period of time would provide a better match. Here we wanted to illustrate the correlation between the instrument data with the reference instrument, when the bike was parked next to the reference site.

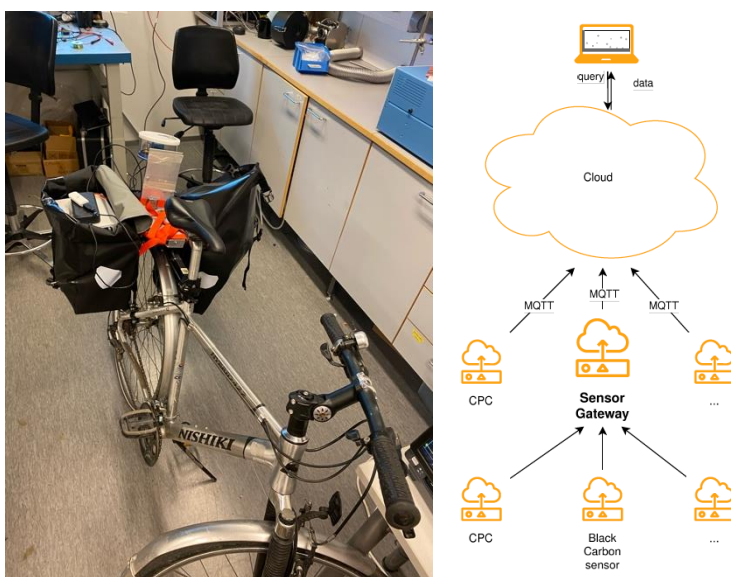


**Figure 31.** The instruments onboard the mobile platform (left) and the data flow (right) connecting the mobile CPC and BC measurements from the bike through a sensor gateway to the cloud, which hosts also the CPC data from fixed observation sites as well. The data can be queried from the cloud for post-processing.

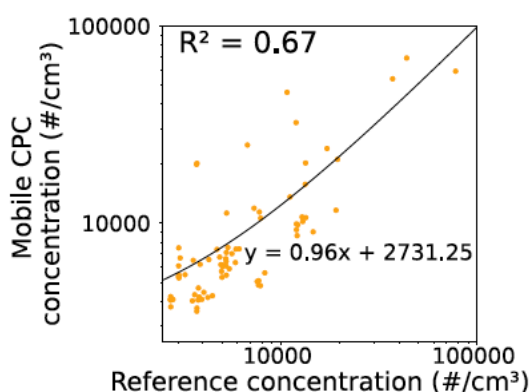


**Figure 32.** Comparison of the experimental CPC data against the reference CPC at SMEAR III observation site during a short 5-min side-by-side measurement.

An exemplary result of the mapping of UFP number concentration in Helsinki is depicted in Figure 33. The measurement route included co-location at two air quality monitoring sites, SMEAR III in urban background and Mäkelänkatu site in urban traffic site. The results indicate high variability in aerosol number concentration. As expected, the highest concentrations were observed near traffic and considerably smaller concentrations were observed in the park areas. The transient nature of the number concentrations are illustrated very well in Mäkelänkatu, where the mobile measurements indicated a gradient between the sides of the street. This is in line with earlier studies with mobile measurements (Pirjola et al. 2012). Within the street canyon the number concentrations are elevated by the local wind patterns inside the street canyon on the leeward side of the prevailing wind. This is due to the local wind structures within the street canyon (Dos Santos-Juusela et al. 2013).

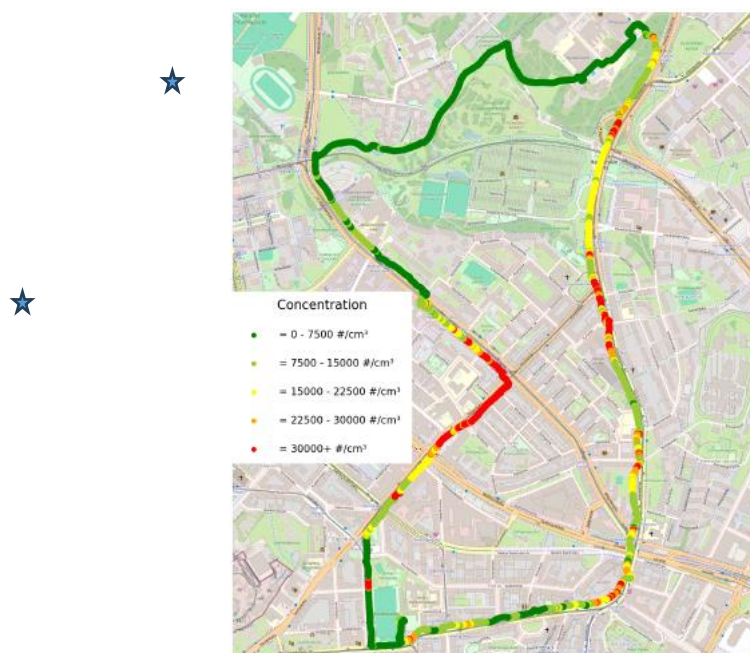


**Figure 33.** Aerosol number concentration in Helsinki region during one exemplary biking exercise. The stars indicate the location of two supersites.

### 9.3 Lessons learned from the Helsinki AQ mapping activities

The lessons learned from the Helsinki pilot are:

- Quality control against the reference instruments is essential. The intercomparison should be done in an ideal case both before and after the campaign. In case of mobile measurements, the intercomparison is recommended during the campaign as well.
- Near-Real time data delivery to the data cloud increases the value and usability of the data. In this manner, the pilot data were connected to operational air quality modeling (e.g. ENFUSER, Johansson et al. 2022) which allowed novel insights into the spatial variability of emerging air pollutants.
- Particularly UPF concentrations are highly variable in the urban environment. Reducing pedestrian exposure to UFPs can be achieved with small changes in their routes through the city.

## 9. Potential for sustainability and upscaling in cities

We discuss the added value of fine resolution monitoring and modelling beyond as complementary tools to data from fixed regulatory Air Quality Monitoring Networks (AQMN) based on the pilot studies. We then discuss whether the approaches used in the pilot studies can be sustainably applied in city air quality networks.

### Added value

Mobile sensing platforms and fixed sensor networks based on low-cost sensors can be used to obtain more fine-spatial resolution pollution data across the city than obtained from routine monitoring stations. In the pilot studies we have especially focused on mobile monitoring with reference grade monitors or more portable monitors that have been shown to compare well with reference grade monitors. The approaches worked well to develop maps across the city, useful for a general assessment for e.g. epidemiological studies. For identifying specific hotspots, more focus on using directly the actually measured concentrations is needed, as was the case for the cycling-based

citizen involved approach in Rotterdam. Monitoring data based on a sufficiently large number of repetitions across the city are useful to identify locations, where current models under- or overestimate concentrations.

Dispersion modelling was useful and agreed well with measurement data from the often few regulatory monitoring stations. Dispersion modelling is probably closer to expertise of network operators, though typically using dispersion models that are applied for regulatory purposes.

Awareness raising, identification of hotspot locations, assessment of exposure during commuting are additional merits of mobile monitoring. A more detailed discussion is found in Deliverable 2.6.

### ***Sustainable implementation***

Mobile monitoring links well to the past practice and expertise of some network agencies, that used mobile monitoring with reference-grade instruments in large vans. This is the approach taken in the Bucharest and Rotterdam car-based mobile monitoring. Supported by adequate QA-QC, a sufficient number of repetitions and a targeted design, monitoring agencies can operate mobile monitoring systems. The investment cost is high, easily exceeding 100,000 Euro, which suggests the approach is only feasible in larger networks. Furthermore, operating costs are moderate to high as a driver is needed. Driving was done by paid students from Rotterdam with no prior knowledge on air pollution monitoring. The measurement car was developed in such a way that the least amount of manual interference is needed with the system. Nevertheless, all drivers were given a one-day training at the start of the campaign. This resulted in almost all measurement days being successful. A challenge for sustainable implementation is the time of day of monitoring. Weekend and evening monitoring is challenging.

Modelling is easier to implement, if prior expertise already exists and input data on emissions are available. A challenge may be the requirements of regulatory modelling, limiting the flexibility of model choice. This applies less to unregulated pollutants such as UFP.

Engagement with citizens in the past decade has been improved because of low-cost sensor networks by citizens, supported by network agencies. Low-cost sensor monitoring is promising to refine spatial resolution and identifying hotspots, provided that quality is controlled. Low-cost monitoring is cheaper and easier to implement than mobile monitoring, when considering only the measurement itself. However, more qualified personnel is needed to process the data and calibrate instruments prior to deployment and on a regularly basis, thereby taking into account threats to quality. The most robust low-cost sensors remain the passive samplers for especially NO<sub>2</sub>, that have proven to be very useful for assessing spatial variation of average exposures (1 week or longer). For many applications long-term average exposure maps are sufficient.

Specific lessons learned for applying these methods have been addressed previously in deliverable 2.6.

## 10. REFERENCES

- Barreira, L. M. F., Helin, A., Aurela, M., Teinilä, K., Friman, M., Kangas, L., Niemi, J. V., Portin, H., Kousa, A., Pirjola, L., Rönkkö, T., Saarikoski, S., and Timonen, H., 2021. In-depth characterization of submicron particulate matter inter-annual variations at a street canyon site in Northern Europe, *Atmos. Chem. Phys.* 21, 6297–6314.
- Baxter, L.K., Dionisio, K.L., Burke, J., Sarnat, S.E., Sarnat, J.A., Hodas, N., Rich, D.Q., Turpin, B.J., Jones, R.R., Mannshardt, E., 2013. Exposure prediction approaches used in air pollution epidemiology studies: key findings and future recommendations. *J. Expo. Sci. Environ. Epidemiol.* 23, 654-659. <http://dx.doi.org/10.1038/jes.2013.62>
- Baruah, A., Bousiotis, D., Damayanti, S., Bigi, A., Ghermandi, G., Ghaffarpasand, O., Harrison, R.M., Pope, F.D., 2024. A novel spatiotemporal prediction approach to fill air pollution data gaps using mobile sensors, machine learning and citizen science techniques. *npj Clim. Atmos. Sci.*, NPJCLIMATSCI-02550R1 (accepted)
- Bousiotis, D., Damayanti, S., Baruah, A., Bigi, A., Beddows, D.C.S., Harrison, R.M., Pope, F.D., 2024. Pinpointing sources of pollution using citizen science and hyperlocal low-cost mobile source apportionment. *Environ. Int.*, 193, 109069, <https://doi.org/10.1016/j.envint.2024.109069>
- Boylan, J.W. and Russell, A.G., 2006. PM and light extinction model performance metrics, goals, and criteria for three-dimensional air quality models. *Atmos. Environ.* 40, 4946-4959. <https://doi.org/10.1016/j.atmosenv.2005.09.087>.
- Dos Santos-Juusela, V., Petäjä, T., Kousa, A. and Hämeri, K., 2013. Spatial - temporal variations of particle number concentrations between a busy street and the urban background, *Atmos. Environ.* 79, 324-333.
- Elomaa, T., Luoma, K., Harni, S., Virkkula, A., Timonen, H., and Petäjä, T., 2024. Applicability of small-scale black carbon sensors to explore high resolution spatial variability of ambient black carbon, *Aerosol Res. Discuss.* <https://doi.org/10.5194/ar-2024-12>.
- Hanna, S. and Chang, J., 2012. Acceptance criteria for urban dispersion model evaluation. *Meteorol. Atmos. Phys.* 116, 133–146. <https://doi.org/10.1007/s00703-011-0177-1>.
- Hari, P., Petäjä, T., Bäck, J., Kerminen, V.-M., Lappalainen, H.K., Vihma, T., Laurila, T., Viisanen, Y., Vesala, T. and Kulmala, M., 2016. Conceptual design of a measurement network of the global change, *Atmos. Chem. Phys.* 16, 21063–21093.
- Järvi, L., Hannuniemi, H., Hussein, T., Junninen, H., Aalto, P., Hillamo, R., Mäkelä, T., Keronen, P., Siivola, E., Vesala, T., and Kulmala, M., 2009. The urban measurement station SMEAR III: Continuous monitoring of air pollution and surface–atmosphere interactions in Helsinki, Finland, *Boreal Environ. Res.* 14, 86-109.
- Johansson, L., Karppinen, A., Kurppa, M., Kousa, A., Niemi, J.V. and Kukkonen, J., 2022. An operational urban air quality model ENFUSER, based on dispersion modelling and data assimilation, *Environ. Model. & Software* 156, 105460.
- Kerckhoffs J, Hoek G, Messier KP, Brunekreef B, Meliefste K, Klompmaker JO, Vermeulen R. Comparison of Ultrafine Particle and Black Carbon Concentration Predictions from a Mobile and Short-Term Stationary Land-Use Regression Model. *Environ Sci Technol.* 2016;50(23):12894-12902.
- Kerckhoffs J, Hoek G, Vlaanderen J, van Nunen E, Messier K, Brunekreef B, Gulliver J, Vermeulen R. Robustness of intra urban land-use regression models for ultrafine particles and black carbon based on mobile monitoring. *Environ Res.* 2017; 159:500-508.

- Kim, Y., Lugon, L., Maison, A., Sarica, T., Roustan, Y., Valari, M., Zhang, Y., André, M., and Sartelet, K., 2022. MUNICH v2.0: a street-network model coupled with SSH-aerosol (v1.2) for multi-pollutant modelling. *Geosci. Model Dev.* 15, 7371–7396, <https://doi.org/10.5194/gmd-15-7371-2022>.
- Kleemola, E., Marsela, A., Haataja, J., Wu, Y., Rohal, D., Koskinen, P., Harni, S., Li, D., Timonen, H., Petäjä, T. and Kangasluoma, J., 2024. Integrated platform for mobile air quality measurements in urban environments, *Proceedings of European Aerosol Conference 2024*, Tampere, Finland.
- Kumar, P., Morawska, L., Martani, C., Biskos, G., Neophytou, M., Di Sabatino, S., Bell, M., Norford, L., Britter, R., March 2015. The rise of low-cost sensing for managing air pollution in cities. *Environ. Int.* 75, 199-205.
- Menut, L., Bessagnet, B., Briant, R., Cholokian, A., Couvidat, F., Mailler, S., Pennel, R., Siour, G., Tuccella, P., Turquety, S., and Valari, M., 2021. The chimere v2020r1 online chemistry-transport model. *Geosci. Model Dev.* 14(11), 6781–6811. <https://doi.org/10.5194/gmd-14-6781-2021>.
- Park, S.J., Lugon, L., Jacquot, O., Kim, Y., Baudic, A., D’Anna, B., Di Antonio, L., Di Biagio, C., Dugay, F., Favez, O., Ghersi, V., Gratien, A., Kammer, J., Petit, J.-E., Sanchez, O., Valari, M., Vigneron, J., Sartelet, K., 2024. Population exposure to outdoor NO<sub>2</sub>, black carbon, particle mass, and number concentrations over Paris with multi-scale modelling down to the street scale. *EGUsphere*, <https://doi.org/10.5194/egusphere-2024-2120>.
- Pirjola, L., Lähde, T., Niemi, J.V., Kousa, A., Rönkkö, T., Karjalainen, P., Keskinen, J., Frey, A., Hillamo, R., 2012. Spatial and temporal characterization of traffic emissions in urban microenvironments with a mobile laboratory. *Atmos. Environ.* 63, 156-167.
- Sartelet, K., Couvidat, F., Wang, Z., Flageul, C., Kim, Y., 2020. SSH-Aerosol v1.1: A modular box model to simulate the evolution of primary and secondary aerosols. *Atmosphere* 11, 525, <https://doi.org/10.3390/atmos11050525>.
- Sartelet, K., Kim, Y., Couvidat, F., Merkel, M., Petäjä T., Sciare J. and Wiedensohler, A., 2022. Influence of emission size distribution and nucleation on number concentrations over Greater Paris. *Atmos. Chem. Phys.* 22, 8579-8596. <https://doi.org/10.5194/acp-22-8579-2022>.
- Savadkoobi, M., Pandolfi, M., Favez, O., Putaud, J.-P., Eleftheriadis, K., Fiebig, M., Hopke, P.K., Laj, P., Wiedensohler, A., Alados-Arboledas, L., Bastian, S., Chazeau, B., María, Á.C., Colombi, C., Costabile, F., Green, D.C., Hueglin, C., Liakakou, E., Luoma, K., Listrani, S., Mihalopoulos, E., Marchand, E., Močnik, G., Niemi, J.V., Ondráček, J., Petit, J.-E., Rattigan, O.V., Reche, C., Timonen, H., Titos, G., Tremper, A.H., Vratolis, S., Vodička, P., Funes, E.Y., Zíková, N., Harrison, R.M., Petäjä, T., Alastuey, A., Querol, X., 2024. Recommendations for reporting equivalent black carbon (eBC) mass concentrations based on long-term pan-European in-situ observations. *Environ. Int.* 185, 108553. <https://doi.org/10.1016/j.envint.2024.108553>.
- Shen Y, de Hoogh K, Schmitz O, Clinton N, Tuxen-Bettman K, Brandt J, Christensen JH, Frohn LM, Geels C, Karsenberg D, Vermeulen R and Hoek G., 2022. Europe-wide air pollution modeling from 2000 to 2019 using geographically weighted regression. *Environ Int.* 107485. doi: 10.1016/j.envint.2022.107485.
- Stocker, J., Hood, C., Carruthers, D. and McHugh, C., 2012. ADMS-Urban: developments in modelling dispersion from the city scale to the local scale. *Int. J. Environ. Pollut.*, 50, 308-316, DOI: 10.1504/ijep.2012.051202.
- Teinilä, K., Saarikoski, S., Lintusaari, H., Lepistö, T., Marjanen, P., Aurela, M., Hellén, H., Tykkä, T., Lampimäki, M., Lampilahti, J., Barreira, L., Mäkelä, T., Kangas, L., Hatakka, J., Harni, S., Kuula, J., Niemi, J. V., Portin, H., Yli-Ojanperä, J., Niemelä, V., Jäppi, M., Lehtipalo, K., Vanhanen, J., Pirjola, L., Manninen, H. E., Petäjä, T., Rönkkö, T., and Timonen, H., 2024 Measurement report: Wintertime aerosol characterization at an urban traffic site in Helsinki Finland, *EGUsphere*, <https://doi.org/10.5194/egusphere-2024-2235>.

- Tilloy, A., V. Mallet, D. Poulet, C. Pesin, and F. Brocheton, 2013. BLUE-based NO<sub>2</sub> data assimilation at urban scale *J. Geophys. Res. Atmos.*, 118, 2031–2040, doi:10.1002/jgrd.50233.
- Van Den Bossche, J., Peters, J., Verwaren, J., Botteldooren, D., Theunis, J. & De Baets, B. 2015. Mobile monitoring for mapping spatial variation in urban air quality: Development and validation of a methodology based on an extensive dataset. *Atmos. Environ.*, 105, 148-161. <https://doi.org/10.1016/j.atmosenv.2015.01.017>